European Journal of Medicinal Chemistry 220 (2021) 113458

Contents lists available at ScienceDirect

European Journal of Medicinal Chemistry

journal homepage: http://www.elsevier.com/locate/ejmech

Palladium-mediated synthesis and biological evaluation of C-10b substituted Dihydropyrrolo[1,2-*b*]isoquinolines as antileishmanial agents

Iratxe Barbolla [a], Leidi Hernández-Suárez [a], Viviana Quevedo-Tumailli [a, b, c], Deyani Nocedo-Mena [a], Sonia Arrasate [a], María Auxiliadora Dea-Ayuela [d], Humberto González-Díaz [a, e, f, ***], Nuria Sotomayor [a, **], Esther Lete [a, *]

[a] Departamento de Química Orgánica e Inorgánica, Facultad de Ciencia y Tecnología, Universidad Del País Vasco / Euskal Herriko Unibertsitatea UPV/EHU, Apdo. 644, 48080, Bilbao, Spain
[b] RNASA-IMEDIR, Computer Science Faculty, University of A Coruña, 15071, A Coruña, Spain
[c] Universidad Estatal Amazónica UEA, Puyo, 160150, Pastaza, Ecuador
[d] Departamento de Farmacia, Facultad de Ciencias de La Salud, Universidad CEU Cardenal Herrera, Edificio Seminario S/n, 46113, Moncada, Valencia, Spain
[e] Basque Center for Biophysics CSIC-UPV/EHU, University of the Basque Country UPV/EHU, 48940, Bilbao, Spain
[f] IKERBASQUE, Basque Foundation for Science, 48011, Bilbao, Spain

ARTICLE INFO

Article history:
Received 15 February 2021
Received in revised form
12 March 2021
Accepted 5 April 2021
Available online 16 April 2021

Keywords:
Leishmaniasis
Pyrroloisoquinoline
Palladium
Cascade reactions
Machine learning
Cheminformatics

ABSTRACT

The development of new molecules for the treatment of leishmaniasis is, a neglected parasitic disease, is urgent as current anti-leishmanial therapeutics are hampered by drug toxicity and resistance. The pyrrolo[1,2-*b*]isoquinoline core was selected as starting point, and palladium-catalyzed Heck-initiated cascade reactions were developed for the synthesis of a series of C-10 substituted derivatives. Their *in vitro* leishmanicidal activity against visceral (*L. donovani*) and cutaneous (*L. amazonensis*) leishmaniasis was evaluated. The best activity was found, in general, for the 10-arylmethyl substituted pyrroloisoquinolines. In particular, **2ad** (IC_{50} = 3.30 μM, SI > 77.01) and **2bb** (IC_{50} = 3.93 μM, SI > 58.77) were approximately 10-fold more potent and selective than the drug of reference (miltefosine), against *L. amazonensis* on *in vitro* promastigote assays, while **2ae** was the more active compound in the *in vitro* amastigote assays (IC_{50} = 33.59 μM, SI > 8.93). Notably, almost all compounds showed low cytotoxicity, CC_{50} > 100 μg/mL in J774 cells, highest tested dose. In addition, we have developed the first Perturbation Theory Machine Learning (PTML) algorithm able to predict simultaneously multiple biological activity parameters (IC_{50}, K_i, *etc.*) *vs.* any *Leishmania* species and target protein, with high values of specificity (>98%) and sensitivity (>90%) in both training and validation series. Therefore, this model may be useful to reduce time and assay costs (material and human resources) in the drug discovery process.

1. Introduction

Leishmaniasis is a neglected parasitic disease, endemic in about 100 countries, with morbidity and mortality increasing daily. The disease is caused by protozoan pathogens of the *Leishmania* genus that are transmitted by sandflies. *Leishmania* spp exists in two morphologically distinct forms: a motile flagellated form (promastigotes) and an intracellular non-flagellated form (amastigotes). There are four main forms of the disease: visceral leishmaniasis (VL, also known as kala-azar); post-kala-azar dermal leishmaniasis (PKDL); cutaneous leishmaniasis (CL); and mucocutaneous leishmaniasis (MCL). While CL is the most common form of the disease, VL is the most serious and can be fatal if untreated [1]. Immunosuppressed patients related to HIV co-infection or solid organ transplantation are prone to infection by *Leishmania*, which can also promote cancer development [2].

* Corresponding author.
** Corresponding author.
*** Corresponding author. Departamento de Química Orgánica e Inorgánica, Facultad de Ciencia y Tecnología, Universidad del País Vasco / Euskal Herriko Unibertsitatea UPV/EHU, Apdo. 644, 48080, Bilbao, Spain.
E-mail addresses: humberto.gonzalezdiaz@ehu.es (H. González-Díaz), nuria.sotomayor@ehu.es (N. Sotomayor), esther.lete@ehu.es (E. Lete).

https://doi.org/10.1016/j.ejmech.2021.113458

Current antileishmanial therapeutics are hampered by drug toxicity, high cost, need for parenteral administration, increasing treatment failure rates, and emergence of Multi-Drug Resistant (MDR) *Leishmania* species or strains. Treatment depends not only on the etiological species and the infection type (CL, VL, PKDL, or MCL), but also on the geographical location where the disease was acquired [3]. Besides, there are few well-validated molecular drug targets in *Leishmania*, but the molecular targets of the current clinical molecules are unknown. VL is treated with different multidrug therapy, different combinations of pentavalent antimonials, paromomycin, liposomal amphotericin B, and miltefosine. Its use is further limited by associated life-threatening toxicities like cardiac arrhythmias, prolonged QT interval (QTc), ventricular premature beats, tachycardia or fibrillation in pentavalent antimonials or nephrotoxicity, hypokalemia and myocarditis in amphotericin B therapy [4]. The toxicity and the narrow therapeutic margin is one of the main limitations of the compounds currently used against leishmaniasis, therefore it is important to search for new therapeutic alternatives that show a reduced toxicity. Moreover, these drugs can have significant side effects, *e.g.* miltefosine can cause birth defects if taken within three months of getting pregnant [5]. On the other hand, treatment of CL should be decided by the clinical lesions, etiological species, the different response to drugs of species and strains, and the possibility to develop into mucosal leishmaniasis [6]. But proven treatments of CL are scarce, being pentavalent antimonials, paromomycin, pentamidine, and the triazol derivative fluconazole the most effective drugs [7] (Fig. 1).

Among the latest advances in this field stand out novel antileishmanial drug-like chemical series based on nitrogen heterocyclic scaffolds, as pyrazolopyrimidine GSK3186899/DDD853651 [8] and benzabenzoxazole derivatives GNF6702 and LXE408 [9] (Fig. 1). Besides, sitamaquine, an 8-aminoquinoline, is a drug candidate for the treatment of VL by oral route, although phase II clinical trials point out some adverse effects, such as methemoglobinemia and nephrotoxicity, which have to be considered for a further development decision [10] (Fig. 1). More recently, 4-aminostyrylquinolines, quinolone-metronidazoles, and ferrocenylquinoline-based derivatives have also shown promising antileishmanial profiles [11]. Currently, identification of new effective and safe antileishmanial drugs is crucial to advance in obtaining new lead compounds and disease control [12].

Our group has experience in the development of synthetic methodologies for the preparation of different benzo(hetero)fused six-membered heterocycles [13], in particular quinoline, isoquinoline and their dihydro counterparts, whose structural cores are among many biologically active natural products and pharmaceuticals [14]. In particular, Lycorane-type of Amaryllidaceae alkaloids may present biological activity against tropical diseases caused by protozoan parasites [15]. On the other hand, Bringmann and Moll have reported that the presence of an aromatic ring linked to the nitrogen atom of the isoquinoline nucleus is crucial for the leishmanicidal activity of these heterocycles [16]. Therefore, we envisioned that the change of the aryl group for an heteroaromatic ring, the pyrrole, but fused to the isoquinoline nucleus by the *b* side, would lead to the pyrrolo[1,2-*b*]isoquinoline core, thus combining structural features of both types of heterocycles.

We recently reported the synthesis of C-10 (hetero)arylmethyl substituted pyrrolo[1,2-*b*]isoquinolines **2** [17] via a Heck/Suzuki cascade reaction (Scheme 1) [18]. Therefore, we decided to explore a palladium-catalyzed intramolecular Heck/anion capture cascade reaction, which would allow to vary the nature of the substituent at

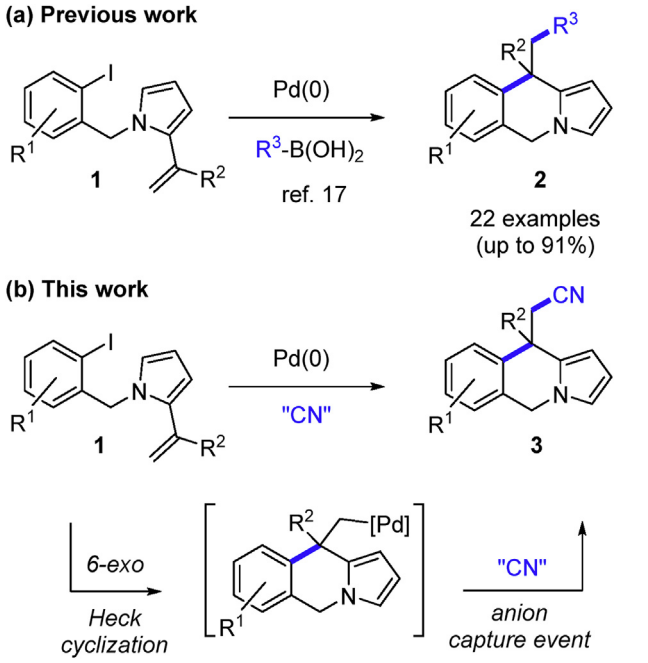

Scheme 1. Synthesis of C-10 substituted pyrrolo[1,2-*b*]isoquinolines **2** and **3** for antileishmanial assays: (a) previously reported Heck/Suzuki cascade; (b) Heck/anion capture cascade.

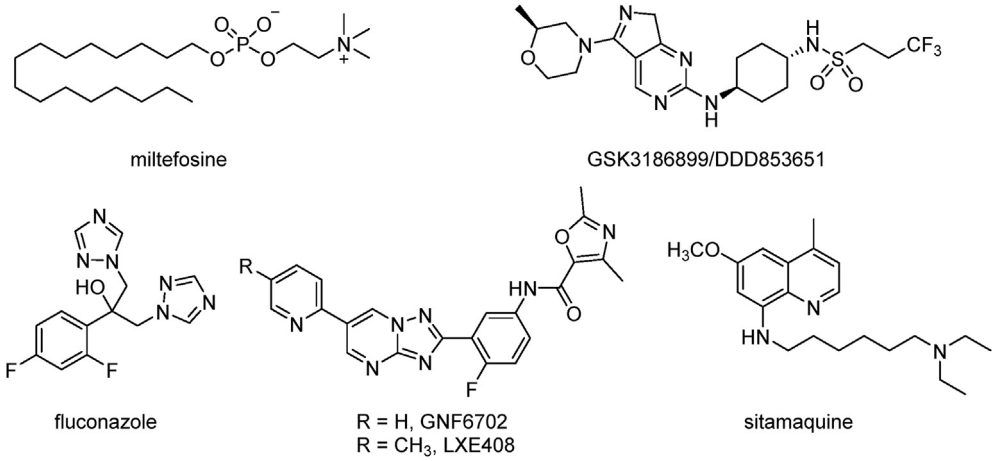

Fig. 1. Antileishmanial drugs with heterocyclic motifs and miltefosine.

C-10b for the study of structure-activity relationships. Thus, intramolecular Heck-type reaction of 2-alkenyl *N*-(*o*-iodobenzyl)pyrroles **1** proceeds *via* an initial 6-*exo* cyclization process to give a σ-alkylpalladium(II) intermediate that would be trapped by a cyanide ion. The use of 1,1-disubstituted alkenes directs the carbopalladation to the most substituted position avoiding the *syn* β-hydride elimination. Thus, the sequential formation of two C–C bonds can be achieved to give pyrrolo[1,2-*b*]isoquinolines **3** with a cyanomethyl substituent at the quaternary stereocenter (Scheme 1).

In this context, Cheminformatics models can be useful to carry out high-throughput computational *in silico* pre-screening of large libraries of compounds. These studies allow to prioritize some families of compounds (potential lead compounds) in the pharmacological assays in order to reduce the time and costs (material and human resources) of the drug discovery process. Thus, assay of new compounds by trial-and-error tests are avoided. Nevertheless, to our best knowledge, there are no reports of computational models for antileishmanial compounds that include data for multiple species and types of assays. The main pitfalls of classic Cheminformatics models are the impossibility to predict simultaneously multiple biological activity parameters of drugs against different target proteins, cell lines, organisms of assay, *etc*. They fail to perform multi-label and multi-output classification of new compounds. Our group has introduced the PTML = Perturbation Theory (PT) + Machine Learning (ML) algorithm to solve similar problems (multiple structures *vs*. multiple species and conditions of assay) in the drug discovery process [19]. PTML models start with a known value (reference) of expected biological activity for a group of compounds or property and add the effect of perturbations (deviations) of the structure and/or conditions of assay of the new case (query compound) with respect to the reference. The PTML approach uses PT Operators (PTOs) such as deviations, moving averages, *etc*. to quantify the effect of these deviations or perturbations over the final biological activity. The simpler PTML models are linear additive models, but more complicated and general PTML models can be constructed. PTML models have been used successfully for predicting different parameters of biological activity and/or toxicity (K_i, IC_{50}, LD_{50}, Km,% inhibition, *etc*.) for the interaction of different compounds with different biological targets (proteins, tissues, cell lines, pathogenic organisms, *etc*.) [20]. Therefore, PTML models are useful to select compounds out of the series to be sent to pharmacological assays.

We describe herein the application of a carbopalladation initiated domino reaction to the synthesis of a series of pyrrolo[1,2-*b*]isoquinoline scaffolds, and their *in vitro* biological evaluation against two species of *Leishmania*, *L. amazonensis* and *L. donovani*, which cause CL and VL, respectively. The effect of varying substitution pattern of the aromatic ring, as well as the nature of the C-10b substituent will be explored. In addition, we have developed the first general-purpose PTML model to predict the antileishmanial activity of these series of pyrroloisoquinolines in different biological assays against different *Leishmania* species.

2. Chemistry

The pyrrolo[1,2-*b*]isoquinolines **3** were synthetized through a intramolecular domino Heck/nucleophile capture anion reaction on 2-alkenyl *N*-(*o*-iodobenzyl)pyrroles **1**, which were prepared following previously reported procedures by us [17]. These Heck/nucleophile capture anion cascade reactions have been mainly applied to the construction of five-membered rings, so our aim will also be to expand the scope of the procedure to the synthesis of six-membered rings. The main challenge was to control the chemoselectivity of the process to favor the initial 6-*exo* carbopalladation over the early coupling of aromatic ring with cyanide ion, so all experimental conditions should be carefully chosen to control the nature of the intermediate palladium(II) species that determine the selectivity.

In these cascade reactions it is crucial to choose, not only the adequate palladium catalyst, but also the cyanide source. Since Grigg's seminal work on palladium catalyzed alkene arylcyanation using KCN as cyanide source [21], the method has been improved. Thus, Neuville and Zhu used $K_4Fe(CN)_6$ in the intramolecular palladium-catalyzed domino Heck/cyanation sequence for the synthesis of a 3,3′-disubstituted oxindole [22]. Later, Lautens reported the diastereoselective synthesis of dihydroisoquinolinones starting from enantiopure *N*-allylcarboxamide with $Zn(CN)_2$ as cyanide source [23]. The same reagent was used in a related Pd-catalyzed dearomative indole bisfunctionalization reaction for the preparation of indolines with congested stereocenters [24].

To test the viability of the method outlined above, we carried out an optimization of the Heck/cyanation reaction conditions on *N*-(*o*-iodobenzyl)pyrrole **1a**. We first explored the reaction with phosphane-free catalytic systems for economical and environmental reasons, testing several cyanation agents. Thus, after examining various pre-catalysts [$Pd(OAc)_2$, $Pd(PPh_3)_4$, $Pd(dba)_2$, $Pd_2(dba)_3{\cdot}CHCl_3$, *etc*.], organic (NEt_3, PMP) and inorganic bases (K_2CO_3, Cs_2CO_3, $NaHCO_3$), polar and non-polar solvents, additives and reaction temperatures, the optimal results were obtained using $Pd(OAc)_2$ (10 mol%) as catalyst, $K_4Fe(CN)_6{\cdot}3H_2O$ (0.22 equiv.) as cyanide source, Na_2CO_3 (1.3 equiv.) as inorganic base and nBu$_4$NCl (1 equiv.) as additive, using a mixture of DMF:H_2O (8:2) as solvent at 120 °C (See Supplementary Material for the details of the optimization of the reaction conditions). It is noteworthy that $K_4Fe(CN)_6{\cdot}3H_2O$ is the best cyanation agent, as it is non-toxic compared with traditional cyanation reagents [KCN, NaCN, $Zn(CN)_2$, TMSCN] and it can easily be handled without special precautions [25]. In addition, substoichiometric amounts of reagent can be used, as all cyanide ions bound to the iron (II) center can be released in the cyanation reaction. In fact, the reaction was slowed (24 h *vs*. 1 h) when using higher amounts of $K_4Fe(CN)_6{\cdot}3H_2O$ (0.44 *vs*. 0.22 equiv.), probably because higher concentration of free cyanide ions in the reaction mixture can form catalytically inactive palladium(II)-cyano complexes that lead to partial catalyst deactivation [26]. Notably, the presence of nBu$_4$NCl as phase-transfer catalyst was essential to shorten the reaction time and to enhance the formation of pyrroloisoquinoline **3a**. In fact, it is known that the addition of tetrabutylammonium halides increases the rates of some steps of the catalytic cycle of the Heck reaction, favoring the 6-*exo*-trig cyclization step [27]. However, the yield is moderate (65%), as the competitive direct cyanation coupling reaction to give **4a** (26%) could not be completely suppressed. The use of a series of phosphane ligands [PPh_3, PtBu$_3$, P(2-furyl)$_3$] did not improve the efficiency of the cascade cyclization of **1a**. Selected examples are shown on Table 1 (See Supplementary Material for more details). Therefore, either using conditions that favor cationic or neutral mechanisms for the *syn* insertion of the Ar–Pd(II)-X complex to the alkene, where the selectivity of the Heck reaction is controlled [28], we could achieve the selective synthesis of the pyrroloisoquinolines **3**.

With an optimized set of conditions in hand, the scope of the Heck/cyanation cascade was examined. Generally, different substitution patterns on the aromatic ring are tolerated, affording the pyrroloisoquinolines **3** in moderate yields, as the direct cyanation process was always competitive (Table 2). Specifically, strongly electron-donating groups as methoxy and methylenedioxy groups (Table 2, entries 3–4 and 7–9) and electron-withdrawing groups (F) (entry 6), as well as unsubstituted derivatives (Table 2, entry 2) were viable under the optimized reaction conditions.

Finally, the cyano group of the pyrrolo[1,2-*b*]isoquinolines **3**

Table 1
Optimization of the carbopalladation/cyanation cascade reaction of **1a**.

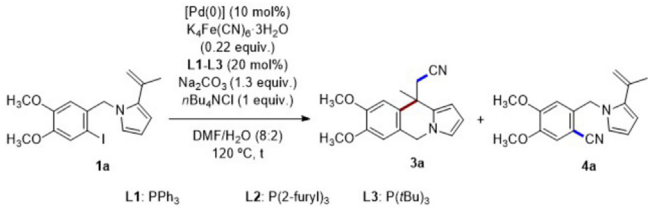

Entry	[Pd]	Ligand	Time (h)	Yield 3a (%)[a]	Yield 4a (%)[a]
1	$Pd(OAc)_2$[b]	_	1	54	32
2	$Pd(OAc)_2$[c]	_	1	65	26
3	$Pd(TFA)_2$[b]	_	4	46	30
4	$Pd(dba)_2$[b]	_	48	37[d]	48
5	$Pd_2(dba)_3 \cdot CHCl_3$[b]	_	48	53[e]	27
6	$Pd(OAc)_2$[c]	**L1**	6	44	40
7	$Pd(OAc)_2$[c]	**L2**	1	52	35
8	$Pd(OAc)_2$[c]	**L3**	24	24	56
9	$Pd(TFA)_2$[c]	**L2**	24	33	31
10	$Pd(dba)_2$[c]	**L2**	6	42	33
11	$Pd_2(dba)_3 \cdot CHCl_3$[c]	**L2**	1	36	39

[a] Isolated yield.
[b] Na_2CO_3 (1 equiv.).
[c] Na_2CO_3 (1.3 equiv.).
[d] Conversion 88%.
[e] Conversion 86%.

Table 2
Carbopalladation/cyanation cascade reaction. Synthesis of **3a-i**.

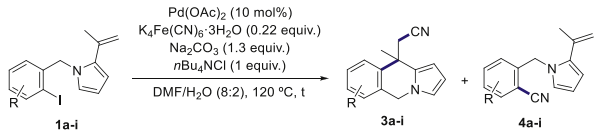

Entry	Ar	Time (h)	Product	Yield (%)[a]	Product	Yield (%)[a]
1	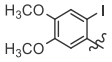	1	**3a**	65	**4a**	26
2		4	**3b**	25	**4b**	41
3		1	**3c**	37	**4c**	38
4	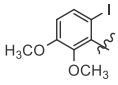	2	**3d**	39	**4d**	29
5	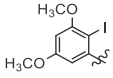	48	**3e**	21[b]	**4e**	-[c]
6		48	**3f**	16	**4f**	18
7	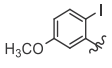	6	**3g**	23[d]	**4g**	28
8	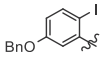	1	**3h**	23	**4h**	15
9	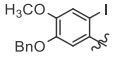	24	**3i**	16	**4i**	30

[a] Yield (%) of isolated pure compound.
[b] Conversion: 63%.
[c] **4e** was detected by ^1H NMR in reaction crude, but it could not be isolated.
[d] Conversion: 94%.

obtained through the domino Heck/cyanation reaction has been efficiently derivatized to different functional groups, such as aldehyde, amide and amine, showing the versatility of the procedure (see Supplementary Material).

3. Antileishmanial assays

The new synthesized 10-cyanomethyl substituted 5,10-dihydropyrrolo[1,2-*b*]isoquinoline derivatives **3**, together with the previously obtained C-10 (hetero)arylmethyl substituted derivatives **2** [17], were screened against two species of *Leishmania*, *L. amazonensis* and *L. donovani*, which cause CL and VL, respectively (Fig. 2). *In vitro* promastigote susceptibility assays and *in vitro* intracellular amastigote susceptibility assays have been carried out, as well as cytotoxicity assay on J774 cell line of macrophages, a line of macrophages used to test cytotoxicity of drugs *in vitro* prior to animal tests (see Experimental Section). Miltefosine was the drug of reference, as it can be used for the treatment of different forms of the disease. The initial screening on the *in vitro* promastigote assays revealed that some 5,10-dihydropyrrolo[1,2-*b*]isoquinolines favorably compare to miltefosine in terms of activity and selectivity against *L. amazonensis*. In general, best activity was found for the 10-arylmethyl substituted derivatives **2aa**, **2ab, 2ad**, **2ae**, **2ag**, **2ah**, **2bb**, and **2db**. In particular, the most active and selective compounds **2ad** (IC_{50} = 3.30 ± 2.80 μM, SI > 77.01) and **2bb** (IC_{50} = 3.93 ± 0.23 μM, SI > 58.77) were approximately 10-fold more potent and selective than the drug of reference (miltefosine), followed by compound **2db** (IC_{50} = 8.00 ± 0.28 μM, SI > 34.4). In contrast, the presence of a cyanomethyl group at C-10 resulted in compounds with weaker antileishmanial activity against *L. amazonensis* (Table 3, entries 12–19). Only compounds **3h** and **3i**, which have an *O*-benzyl group at the 7-position of the pyrroloisoquinoline core, have an activity against *L. amazonensis* comparable to that of miltefosine (Table 3, entries 18–19 *vs.* entry 20). Therefore, the presence of a benzyl group in the pyrroloisoquinoline core seems to be crucial for the antileishmanial activity.

The aromatic substitution pattern of the pyrroloisoquinoline core of this series **2** also plays an important role, having the electron-donating substituents a positive impact on antileishmanial activity against *L. amazonensis*. Thus, compound **2cb**, with an unsubstituted aromatic ring, is 4-47-fold less potent than other compounds of series **2** (Table 3, entry 10 *vs.* entries 1 and 11). Besides, as shown in Table 3, replacement of the methyl group at the 10-position of the pyrroloisoquinoline ring system by a trifluoromethyl group resulted in more active compounds, being **2bb** over 4-fold more active against *L. amazonensis* than **2ab** (Table 3, entry 2 *vs.* entry 9). Regarding the substitution pattern of the benzyl moiety, the presence of two trifluoromethyl groups was detrimental for activity and selectivity, being **2ac** the less active and more toxic derivative of both series (Table 3, entry 3). However, it should be pointed out that the introduction of this CF_3 group at C-10 has less effect (Table 3, entry 2 *vs.* entry 9).

Conversely, all pyrroloisoquinolines tested are notably less active than miltefosine for the treatment of *L. donovani*, being again compound **2bb** one of the more active and selective of both series with IC_{50} = 16.41 ± 4.90 μM and SI > 14.09. In addition, and very notably, almost all pyrroloisoquinolines are much less toxic than the drug of reference with values of concentration of the compound that produces 50% reduction of cell viability (Cytotoxic Concentration, CC_{50}) in the range 195–416 μM in J774 cells. In fact, the Selectivity Index (SI = CC_{50}/IC_{50}) is higher for almost all pyrroloisoquinolines than for miltefosine whose SI is only 4.43. It also should be pointed out that although better IC_{50} values have been reported for different types of molecules against different *Leishmania* species [29], they usually have lower CC_{50} values than most

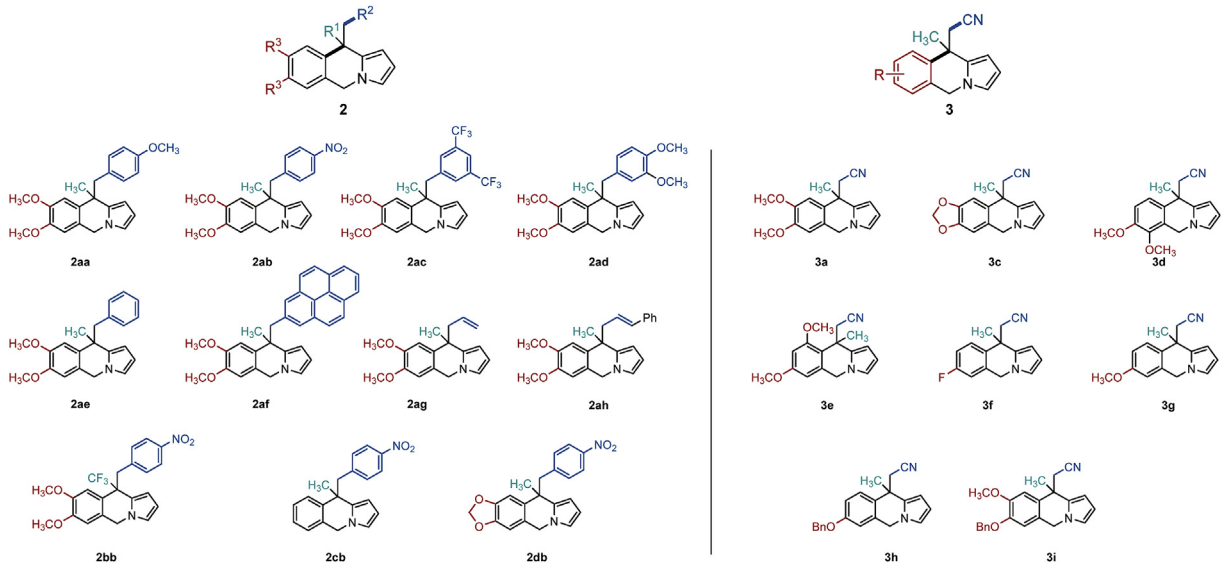

Fig. 2. C-10 substituted 5,10-dihydropyrrolo[1,2-*b*]isoquinolines **2** and **3** screened against *L. amazonensis* and *L. donovani*.

Table 3
IC_{50} leishmanicidal and cytotoxic effects from pyrroloisoquinoline derivatives (expressed as μM) on *in vitro* promastigote assay.

Entry	Comp.	*L. amazonensis*		*L. donovani*		Macrophages J774
		IC_{50} ± SD (μM)[a]	SI[b]	IC_{50} ± SD (μM)[a]	SI[b]	CC_{50} ± SD (μM)[c]
1	**2aa**	26.41 ± 2.20	>10.40	47.40 ± 1.79	>5.80	≥275.13[e]
2	**2ab**	18.00 ± 0.79	>14.68	79.93 ± 4.36	>3.31	≥264.24[e]
3	**2ac**	39.62 ± 2.13	1.18	111.34 ± 10.8	0.42	46.80 ± 4.00
4	**2ad**	3.30 ± 2.80	>77.01	38.30 ± 3.36	>6.63	≥254.14[e]
5	**2ae**	17.09 ± 0.60	>17.54	30.29 ± 2.01	>10.09	≥299.91[e]
6	**2af**	36.71 ± 0.44	>5.95	86.01 ± 1.60	>2.54	≥218.54[e]
7	**2ag**	23.29 ± 1.41	>15.15	124.43 ± 14.70	>2.84	≥352.89[e]
8	**2ah**	12.24 ± 0.56	>23.00	33.66 ± 2.06	>8.27	≥278.20[e]
9	**2bb**	3.93 ± 0.23	>58.77	16.41 ± 4.90	>14.09	≥231.30[e]
10	**2cb**	157.35 ± 6.28	>2.00	159.40 ± 26.20	>1.97	≥314.09[e]
11	**2db**	8.00 ± 0.28	>34.49	30.35 ± 3.92	>9.09	≥275.95[e]
12	**3a**	309.20 ± 41.10	>1.14	226.21 ± 11.60	>1.57	≥354.18[e]
13	**3c**	77.35 ± 1.13	>4.85	120.12 ± 12.01	>3.13	≥375.51[e]
14	**3d**	171.07 ± 6.38	>2.07	nd[d]	nd[d]	≥354.18[e]
15	**3e**	93.85 ± 6.02	>3.77	nd[d]	nd[d]	≥354.20[e]
16	**3f**	96.55 ± 1.66	>4.31	192.19 ± 7.66	>2.17	≥416.18[e]
17	**3g**	123.25 ± 10.70	>3.21	359.99 ± 34.44	>1.10	≥396.32[e]
18	**3h**	15.83 ± 0.06	14.04	60.25 ± 0.34	3.69	222.30 ± 42.70
19	**3i**	24.82 ± 0.28	7.86	34.37 ± 5.30	5.68	195.30 ± 27.30
20	miltefosine	30.70 ± 0.98	4.43	0.15 ± 0.02	906.00	135.90 ± 10.30

[a] IC_{50}: Concentration of the compound that produced a 50% reduction in parasites; SD: Standard Deviation.
[b] SI: Selectivity Index, SI = CC_{50}/IC_{50}.
[c] CC_{50}: Concentration of the compound that produced a 50% reduction of cell viability in treated culture cells with respect to untreated ones.
[d] nd: not determined.
[e] CC_{50} values, expressed as μM, correspond to 100 μg/mL, which was the higher doses tested.

of our pyrroloisoquinolines, which are not toxic at the highest tested dose (CC_{50} > 100 μg/mL). Therefore, this is a very interesting result, considering that currently available chemotherapy for leishmaniasis is hampered by toxicity and drug resistance.

Then, the most active compounds of the promastigote assays were screened against amastigotes of *L. amazonensis* and *L. donovani* (Table 4). All pyrroloisoquinolines tested were less active than miltefosine when tested against *L. donovani* amastigotes. However, these compounds have IC_{50} values in the range 33.59–77.12 μM, which are similar or even better than miltefosine (IC_{50} = 47.60 ± 7.04 μM) in the test against *L. amazonensis*. All of them have SI values between 3.58 and 8.93, which are 2- to 4-fold higher than miltefosine (SI = 2.85). In this case, pyrroloisoquinoline **2ae** showed the best activity with IC_{50} = 33.59 ± 2.64 μM and higher selectivity with SI > 8.93.

We can observe that 10-arylmethyl substituted dihydropyrroloisoquinoline series seems to be more selective and presents similar or even better activity than the drug of reference for the treatment of *L. amazonensis* amastigotes. The result is promising because in the present model of experimental assay the amastigotes are inside the human macrophage cells. Therefore, it seems that these pyrroloisoquinolines could be able to cross/attached host and parasite barriers to exert their activity without damaging the host membrane (macrophage membrane). First, they need to cross the membrane of the host cells (macrophages), next they need to cross Parasitophorous Vacuole Membrane (PVM). Last, if the activity is not over PVM directly, the compounds should reach/cross the parasite membrane to reach their molecular target in the membrane or inside the parasite. The PVM prevents the acidification of the media by lysosomes of the host cell to destroy an

Table 4
IC_{50} Leishmanicidal and cytotoxic effects from pyrroloisoquinoline derivatives (expressed as μM) on *in vitro* amastigote assay.

Entry	Compound	*L. amazonensis*		*L. donovani*		Macrophages J774
		IC_{50} ± SD (μM)[a]	SI[b]	IC_{50} ± SD (μM)[a]	SI[b]	CC_{50} ± SD (μM)[c]
1	**2aa**	51.56 ± 12.00	>5.34	45.00 ± 7.51	>6.12	≥275.13[e]
2	**2ab**	56.12 ± 13.50	>4.70	29.62 ± 6.87	>8.92	≥264.24[e]
3	**2ad**	60.79 ± 5.74	>4.18	46.30 ± 0.33	>5.49	≥254.14[e]
4	**2ae**	33.59 ± 2.64	>8.93	55.03 ± 3.96	>5.45	≥299.91[e]
5	**2ag**	43.54 ± 9.53	>8.10	255.88 ± 42.10	>1.38	≥352.89[e]
6	**2ah**	69.26 ± 6.96	>4.02	16.74 ± 0.14	>16.61	≥278.20[e]
7	**2bb**	56.72 ± 4.58	>4.08	22.17 ± 4.16	>10.43	≥231.30[e]
8	**2db**	77.12 ± 19.10	>3.58	68.65 ± 9.63	>4.02	≥275.95[e]
9	**3h**	nd[d]	_	44.75 ± 8.53	4.97	222.30 ± 42.70
10	miltefosine	47.60 ± 7.04	2.85	0.37 ± 0.05	369.30	135.90 ± 10.30

[a] IC_{50}: Concentration of the compound that produced a 50% reduction in parasites; SD: Standard Deviation.
[b] SI: Selectivity Index, SI = CC_{50}/IC_{50}.
[c] CC_{50}: Concentration of the compound that produced a 50% reduction of cell viability in treated culture cells with respect to untreated ones.
[d] nd: not determined.
[e] CC_{50} values, expressed as μM, correspond to 100 μg/mL, which was the higher doses tested.

invading parasite. PVM is shaped by the parasite using parts of the membrane of the host cell. The PVM surrounds the intracellular parasite, creating a separate bubble of cytoplasm-filled plasma membrane within the host cell [30].

4. Computational model

As described above, we have measured the experimental IC_{50}(μM) values for the series of pyrroloisoquinolines **2** and **3** from the tests against two species of *Leishmania*, *L. amazonensis* and *L. donovani*, at two different stages (S) of development of the parasite: amastigotes (A) and promastigotes (P). We could observe a certain tendency in the behavior of these pyrroloisoquinolines against the promastigotes of the two different species of *Leishmania* studied. In fact, we found a regression coefficient of R = 0.67 for the IC_{50} of pyrroloisoquinoline derivatives in *L. amazonensis vs. L. donovani*. However, we have not yet clues about the possible target proteins of these compounds. In addition, there are many other species of *Leishmania* (including MDR strains) that could not be assayed and may present different susceptibilities to the same drugs.

In order to put our results into context, a ChEMBL dataset of >145,000 preclinical assays of putative antileishmanial compounds was downloaded and explored, as detailed in Experimental Section and the Supplementary Material. The experiments include up to 10 different conditions of assay $c_j = [c_0, c_1, c_2, \ldots c_{10}]$, which were split into two partitions or subsets of experimental conditions c_I and c_{II}. The principal conditions c_I are those that characterize the biological experiment *per se* (parameter measured, target protein, parasite stage, organism of assay, *etc.*). The dataset includes values for $n(c_0) > 50$ different biological parameters measured for compounds *vs.* at least one out of $n(c_1) = 32$ target proteins, $n(c_2) = 29$ cell lines, $n(c_3) = 40$ organisms of assay (not all are parasites), and $n(c_4) = 37$ *Leishmania* parasite species or strains, *etc.* Instead of outcomes for all possible experiments, the dataset includes $n(c_I) > 240$ combinations of these principal conditions c_I (different experiments) for numerous compounds. In addition, the dataset includes $n(c_{II}) = 80$ combinations of secondary c_{II} conditions related to the biological nature and/or accuracy of data (target type, target mapping, value exactitude, *etc.*). This study revealed that above 70 assays involving 20 species/strains of *Leishmania* are most commonly used. Unfortunately, even limiting the analysis to these assays it may be costly in terms of resources and time. Testing a short series of only 10 compounds would require $n_{assay} = 10 \cdot 70 = 700$ experimental assays. Therefore, we decided to carry out a preliminary computational study of the susceptibility of other species to this series of compounds. As stated above, there are no reports on a computational model to perform such study. Therefore, we first developed a new PTML model to carry out this type of predictions. The equation of the best PTML model found is the following:

$$f(v_{ij})_{calc} = 59.918599 \cdot f(v_{ij})_{ref} + 1.631537 \cdot \Delta D_1(c_I) + 0.041494 \cdot \Delta D_2(c_I) - 2.675709 \cdot \Delta D_3(c_I) - 1.562187 \cdot \Delta D_1(c_{II}) - 0.041886 \cdot \Delta D_2(c_{II}) + 2.649511 \cdot \Delta D_3(c_{II}) - 25.182671$$

$$n = 109389 \quad \chi^2 = 135169.7 \quad p < 0.05$$

The idea of this PTML model is to start using as input a function of reference $f(v_{ij})_{ref}$, which is obtained from the experimental assays of a set of compounds of reference carried out under specific conditions c_j. This function quantifies the expected prior probability to give a positive result in the specific assays for a compound selected at random. Next, the values of the PT Operators (PTOs) with the general form $\Delta D_k(c_j)$ were added to the $f(v_{ij})_{ref}$. These PTOs quantify the deviation (Δ) of the molecular descriptors D_k (structure) of our query compound with respect to the group of reference compounds (see Experimental Section). The descriptors D_k are D_1 = ALOGP, the *n*-octanol/water partition coefficient, D_2 = TPSA, the Topological Polar Surface Area, and D_3 = NRV, the Number of Violations to Rule of V (Lipinski's or Pfizer's rule) were used to identify each compound in the equation. The descriptors ALOGP and TPSA quantify the molecular structure of the drug by means of a weigthed sum of different molecular fragments in the molecules. NRV rule quantifies the likeness/similarity of one compound with respect to known drugs based on molecular weight, hydrogen bonds, *etc.* [31]. The values of D_k were extracted from ChEMBL dataset and/or calculated with the software DRAGON for new compounds. Finally, the output of the model $f(v_{ij})_{calc}$ is a scoring function used to calculate the probability of activity $p(f(v_{ij})_{pred} = 1)$ of different compounds. In order to train this model, we selected at random a large training series of n = 109,389 preclinical assays downloaded from ChEMBL database. The values of Specificity (Sp) and Sensitivity (Sn) are in the range ≈ 90–98% for training series (see Supplementary Material), which are excellent values for this type of ML classification models. Moreover, the p-level < 0.05 for the Chi-square test with χ^2 = 135,169.7 points to a statistically significant discrimination

between active ($f(v_{ij})_{obs} = 1$) and non-active compounds ($f(v_{ij})_{obs} = 0$) in all these assays. This model may be used to predict new compounds not included in training series. First, the values of the $f(v_{ij})_{ref}$ and PTOs (containing D_k of drug and $<D_k(c_j)>$ of assay) were substituted in the equation to calculate the output function $f(v_{ij})_{calc}$. Next, the values of $f(v_{ij})_{calc}$ were transformed into posterior probabilities of success $p(f(v_{ij})_{pred} = 1)$ for each compound in different assays using a sigmoid function. Once the values of probabilities were calculated, the compounds could be classified. Thus, those outcomes in the range of probability $p(f(v_{ij})_{pred} = 1) > 0.5$ are considered interesting for assay $f(v_{ij})_{pred} = 1$. Then, the present PTML model was tested with a very large validation series, obtaining values of Sp and Sn also in the range ≈ 90–98% for the external validation series. In conclusion, this simple but powerful PTML model predicts very well (overall Accuracy = 97.8%) a large dataset (training + validation) of anti-leishmanial activity preclinical assays ($n_{assay} > 145{,}000$) involving 96,800 unique compounds.

5. Predictive study

As mentioned above, some compounds of our series show interesting IC_{50} values and can be considered active ($f(v_{ij}) = 1$)) using the cutoff of $IC_{50} = 10$ μM in the range of more typical experimental studies. Then, we decided to use this new model to carry out a computational prediction of the outcomes of the 19 pyrroloisoquinolines of our series *vs*. different *Leishmania* species (>20) in more than 160 different preclinical assays. This PTML model is able to predict the posterior probability $p(f(v_{ij})_{pred} = 1)$ of getting the desired level for more than 50 different biological properties (IC_{50}, K_i, K_m, *etc.*). In this preliminary study, IC_{50} was selected as unique property, as it was the first property experimentally measured in the early stages of screening, using a very low cut-off value of $IC_{50} = 0.01$ μM, in an effort to reduce the number of false positive cases from the first steps of screening. Consequently, the model was used to calculate the values of probability $p(IC_{50}(\mu M) < 0.01)_{calc}$ for which a compound would show an $IC_{50}(\mu M) < 0.01$ in different assays. The total number of calculations for *in vitro* assays that do not specify the target protein was $n_{calc1} = n_{cmpd} \cdot n_{assay} = 19 \cdot 162 = 3078$. The full results of this predictive study are compiled in Table S9 of the Supplementary Material. The values of $p(IC_{50}(\mu M) < 0.01)_{calc}$ for assays with known protein targets were also predicted, being the number of calculations $n_{calc2} = n_{cmpd} \cdot n_{prot} = 19 \cdot 32 = 608$ for the 19 compounds *vs*. 32 target proteins of different species. It makes a total of $n_{calc} = n_{calc1} + n_{calc2} = 3686$ calculations for our 19 compounds in different assays. For the sake of simplicity, we only changed the conditions c_I (assay *per se*) using a fix sub-set of conditions c_{II} for the 3686 calculations. Consequently, the total number of predicted values of $p(IC_{50}(\mu M) < 0.01)_{calc}$ was 3686. In order to summarize the results and withdraw conclusions, we calculated the average value of the probability $p(IC_{50}(\mu M) < 0.01)_{avg}$, which is the average probability that the compound is predicted to have an $IC_{50}(\mu M) < 0.01$ in multiple assays *vs*. the same species. The PTML model predicts a coherent behavior for this series of compounds as a homologous series. It means that species resistant/susceptible to one compound are predicted to be resistant to the action of almost all compounds of the whole series. The model does not detect overall significant differences on the behavior of both subseries (**2aa-2db** *vs*. **3a-3i** subseries) of compounds, which could be coherent with the fact that both subseries of compounds have the pyrroloisoquinoline core. The average value of probability $p(IC_{50}(\mu M) < 0.01)_{avg}$ for almost all compounds of the series are in the range 0.1–0.4, $p(IC_{50}(\mu M) < 0.01) < 0.5$, for many species of *Leishmania*, which is in agreement with the experimental findings.

Table 5 shows selected results of the predictive study *vs*. different species for the two top lead compounds of each subseries (**2ad**, **2bb**, **3h**, and **3i**) experimentally tested in this work (see Supplementary Material for full details). Interestingly, the PTML model predicts values of $p(IC_{50}(\mu M) < 0.01)_{avg} > 0.8$ for some species/strains not previously tested, despite of the demanding computational threshold value used in the computational study. See, for example, the values of $p(IC_{50}(\mu M) < 0.01)_{avg}$ of the four top hit compounds for *L. braziliensis strain M2904* (*L. brm.*), and *L. major strain Friendlin* (*L. maf.*), and *L. mexicana (L. mex.),* shown in Table 5. Regarding the possible target protein, the model predicts values of $p(IC_{50}(\mu M) < 0.01)_{avg} > 0.7$ for both subseries of pyrroloisoquinolines *versus* some proteins. The study points to the Trypanothione reductase of *L. donovani* (P39050) [32], L-isoaspartate(D-aspartate) *O*-methyltransferase (P22061) of *L. donovani* [33] and the Ornithine decarboxylase of *L. donovani* (P27116) [34] as plausible targets to be tested, although more candidates are also collected in Table 5. It is interesting that some of these proteins are enzymes with amino acid derivatives (Trypanothione, D-aspartate, and Ornithine) as substrates. Therefore, this computational study opens the door to a further testing of these compounds or their derivatives *vs*. other species of *Leishmania* and specific tests *vs.* probable protein targets.

6. Conclusions

In conclusion, the palladium-catalyzed Heck-initiated cascade reactions are effective procedures for the construction of the pyrrolo[1,2-*b*]isoquinoline scaffolds with a quaternary center at C-10b. The *in vitro* evaluation of their leishmanicidal activity against visceral (*L. donovani*) and cutaneous (*L. amazonensis*) leishmaniasis revelead that almost all compounds showed very low cytotoxicity, $CC_{50} > 100$ μg/mL in J774 cells (highest tested dose). This is an important feature, as drug toxicity is one of the main limitations of current chemotherapy for leishmaniasis. In general, 10-arylmethyl substituted pyrroloisoquinolines showed best activity against *L. amazonensis* on *in vitro* promastigote assays. In particular, **2ad** ($IC_{50} = 3.30$ μM, SI > 77.01) and **2bb** ($IC_{50} = 3.93$ μM, SI > 58.77) were approximately 10-fold more potent and selective than the drug of reference (miltefosine). On the other hand, **2ae** was the more active compound in the *in vitro* amastigote assays ($IC_{50} = 33.59$ μM, SI > 8.93). In addition, it has been demonstrated that Perturbation Theory Machine Learning (PTML) algorithms are useful to model large (>145,000 cases) ChEMBL datasets of anti-leishmanial preclinical assays. It is possible to use the developed PTML model to reduce assay costs by predicting the probability with which a query compound of this or other series of compounds reaches a desired level for multiple parameters (IC_{50}, K_i, *etc.*) *vs*. different *Leishmania* species and target proteins, with high values of specificity (>98%) and sensitivity (>90%) in both training and validation series.

7. Experimental section

7.1. Chemistry

General. All commercial chemicals were reagent grade and were used without further purification unless otherwise specified. Palladium catalysts were commercially available, and were used without further purification: $Pd(OAc)_2$: 98% purity; $Pd(TFA)_2$: 97% purity; $Pd(PPh_3)_4$: 99% purity.; $Pd(dba)_2$: 99.9% purity; $Pd_2(dba)_3 \cdot CHCl_3$: 97% purity. The 1-(*o*-iodobenzyl)-2-alkenylpyrroles **1** were synthetized according to the procedures previously reported by us [17]. All solvents used in reactions were anhydrous and purified according to standard procedures. All air- or moisture-sensitive reactions were performed under argon; the

Table 5
PTML prediction of average value of probability $p(IC_{50}(\mu M) < 0.01)_{avg}$ for pyrroloisoquinolines **2ad**, **2bb**, **3h**, and **3i** against > 20 different *Leishmania* species.

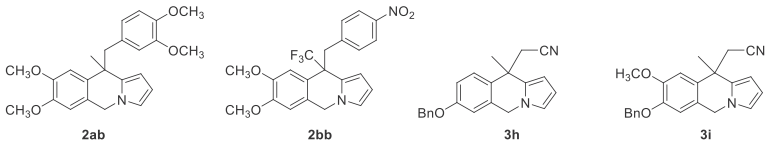

Leish.	S[b]	Target	Compound				*Leish.*	S[b]	Target	Compound			
Species		Protein	2ad	2bb	3h	3i	*Species*[a]		Protein	2ad	2bb	3h	3i
L. aet.	A	_	0.02	0.01	0.01	0.01	*L. maj.*	_	P37268	0.41	0.34	0.30	0.32
L. aet.	P	_	0.02	0.01	0.01	0.01	*L. maj.*	_	Q01782	0.58	0.51	0.47	0.49
L. ama.	A	_	0.10	0.08	0.06	0.07	*L. maj.*	_	Q0GKD7	0.43	0.36	0.32	0.34
L. ama.	P	_	0.21	0.17	0.15	0.15	*L. maj.*	_	Q4Q5S8	0.04	0.03	0.03	0.03
L. ama.	_	O96394	0.64	0.58	0.53	0.55	*L. maj.*	_	Q4Q5W4	0.78	0.73	0.69	0.71
L. ari.	_	_	0.21	0.17	0.15	0.16	*L. maj.*	_	Q4QBL1	0.52	0.46	0.41	0.43
L. bra.	A	_	0.12	0.09	0.08	0.09	*L. maj.*	_	Q4QE15	0.02	0.02	0.01	0.02
L. bra.	P	_	0.20	0.16	0.14	0.15	*L. maj.*	_	Q6S996	0.17	0.13	0.11	0.12
L. brm.	A	_	0.93	0.91	0.89	0.90	*L. maj.*	_	Q9LM02	0.04	0.03	0.02	0.03
L. brm.	P	_	0.11	0.09	0.07	0.08	*L. maj.*	P	_	0.06	0.05	0.04	0.05
L. cha.	A	_	0.18	0.15	0.13	0.14	*L. maj.*	P	Q01782	0.41	0.35	0.31	0.33
L. cha.	P	_	0.25	0.21	0.18	0.19	*L. maf.*	P	_	0.94	0.92	0.90	0.91
L. don.	A	_	0.30	0.27	0.25	0.25	*L. mex.*	A	_	0.30	0.26	0.24	0.25
L. don.	_	P39050	0.83	0.79	0.76	0.77	*L. mex.*	_	P04406	0.73	0.67	0.63	0.65
L. don.	_	Q95WR6	0.16	0.13	0.11	0.12	*L. mex.*	_	P36400	0.35	0.29	0.26	0.27
L. don.	_	Q95Z89	0.29	0.24	0.21	0.22	*L. mex.*	_	Q01558	0.60	0.54	0.50	0.51
L. don.	_	Q9NJG8	0.07	0.05	0.04	0.05	*L. mex.*	_	Q27686	0.96	0.95	0.95	0.95
L. don.	P	_	0.25	0.23	0.22	0.23	*L. mex.*	_	Q4U254	0.41	0.35	0.31	0.32
L. don.	P	P22061	1.00	1.00	1.00	1.00	*L. mex.*	_	Q9U5N6	0.34	0.28	0.25	0.26
L. don.	P	P27116	1.00	0.99	0.99	0.99	*L. mex.*	P	_	0.27	0.22	0.20	0.21
L. dod.	_	_	0.21	0.17	0.15	0.16	*L. mex.*	P	P11166	0.09	0.07	0.06	0.06
L. enr.	P	_	0.13	0.10	0.09	0.09	*L. mem.*	_	Q27686	0.29	0.24	0.21	0.22
L. gar.	_	_	0.21	0.17	0.15	0.16	*L. mem.*	P	_	0.02	0.01	0.01	0.01
L. guy.	A	_	0.08	0.06	0.05	0.06	*L. mev.*	_	_	0.21	0.17	0.15	0.16
L. guy.	P	_	0.28	0.23	0.20	0.21	*L. pan.*	A	_	0.10	0.08	0.07	0.07
L. inf.	A	_	0.32	0.28	0.26	0.27	*L. pan.*	P	_	0.42	0.38	0.35	0.36
L. inf.	_	Q8I6E4	0.28	0.23	0.20	0.21	*L. per.*	P	_	0.23	0.19	0.16	0.17
L. inf.	P	_	0.20	0.17	0.15	0.15	*L. pif.*	A	_	0.11	0.09	0.07	0.08
L. maj.	A	_	0.23	0.20	0.18	0.18	*L. pif.*	P	_	0.21	0.17	0.14	0.15
L. maj.	_	O15826	0.76	0.70	0.67	0.68	*L. pro.*	P	_	0.11	0.09	0.07	0.08
L. maj.	_	O96526	0.07	0.06	0.05	0.05	*L. tar.*	_	_	0.10	0.08	0.07	0.07
L. maj.	_	P00374	0.21	0.17	0.15	0.16	*L. tro.*	P	_	0.18	0.14	0.12	0.13
L. maj.	_	P07382	0.22	0.18	0.16	0.16	*L. tur.*	_	_	0.08	0.06	0.05	0.05

[a] *Leishmania* species: *L. aethiopica* = *L. aet.*, *L. amazonensis* = *L. ama.*, *L. aristidesi* = *L. ari.*, *L. braziliensis* = *L. bra.*, *L. braziliensis M2904* = *L. brm*, *L. chagasi* = *L. cha.*, *L. donovani* = *L. don.*, *L. donovani donovani* = *L. dod.*, *L. enriettii* = *L. enr.*, *L. garnhami* = *L. gar.*, *L. guyanensis* = *L. guy*, *L. infantum* = *L. inf.*, *L. major* = *L. maj.*, *L. Mexicana* = *L. mex.*, *L. mexicana mexicana* = *L. mem.*, *L. mexicana venezuelensis* = *L. mev.*, *L. panamensis* = *L. pan.*, *L. peruviana* = *L. per.*, *L. pifanoi* = *L. pif.*, *L. tarentolae* = *L. tar.*, L. tropica = *L. tro.*, L. turanica = *L. tur.*, *L. major strain Friendlin* = *L. maf.*
[b] S = Stage: A = Amastigotes, P = Promastigotes.

glassware was dried (130 °C) and purged with argon. TLC was carried out with 0.2 mm-thick silica gel Merck F254 plates. Visualization was accomplished by UV light (λ = 254 nm and 360 nm). Flash column chromatographic separations and purifications were performed on silica Flash P60 (Silicycle), 230–400 mesh ASTM. Final compounds were purified to ≥95% purity as assessed by ^{1}H NMR spectra and analytical liquid chromatography. Melting points were measured in a Büchi B-540 apparatus in unsealed capillary tubes. IR spectra were obtained using Attenuated Total Reflection (ATR) in a JASCO FT/IR 4100 in the interval between 4000 and 400 cm^{-1} with a 4 cm^{-1} resolution. Only characteristic bands are given in each case. ^{1}H and ^{13}C NMR spectra were recorded at 20–25 °C on either a Bruker AC-300 spectrometer (300 MHz for ^{1}H and 75.5 MHz for ^{13}C) and on a Bruker AC-500 spectrometer (500 MHz for ^{1}H and 125.7 MHz for ^{13}C). Chemical shifts are reported in parts per million (ppm) relative to an internal solvent reference. Recorded peaks are listed in the order multiplicity (s, singlet; d, doublet; dd, doublet of doublets; m, multiplet), coupling constants, and number of protons. Assignments of individual ^{13}C and ^{1}H resonances are supported by DEPT experiments and 2D correlation experiments (COSY, HSQCed or HMBC) when necessary. High resolution mass spectra (HRMS) were performed by the Mass Spectrometry General Service at the University of the Basque Country using an ultra performance liquid chromatograph (Acquity UPLC, Waters Chromatography.), in tandem with a QTOF mass spectrometer (SYNAPT G2 HDMS, Waters Chromatography), with an electrospray ionization source in a positive mode.

Intramolecular Heck/cyanide capture cascade reaction on 1. Synthesis of pyrrolo[1,2-*b*]isoquinolines 3. General procedure. $Pd(OAc)_2$ (0.1 mmol) was added to a mixture of *N*-(*o*-iodobenzyl) pyrrole **1** (1 mmol), potassium hexacyanoferrate(II) trihydrate (0.22 mmol), sodium carbonate (1.3 mmol), and tetrabutylammonium chloride (1 mmol) in an 8/2 mixture of DMF/H_2O (3 mL). The mixture was stirred at 120 °C for the time indicated in each case. H_2O (15 mL) was added and the resulting aqueous phase was extracted with EtOAc (3 × 20 mL). The combined organic extracts were washed with brine (3 × 20 mL), dried over anhydrous Na_2SO_4 and concentrated *in vacuo*. Purification by column chromatography (silica gel) of the resulting residue afforded the corresponding pyrroloisoquinoline **3** and direct aryl halide cyanation product **4** (see Supplementary Material).

2-(7,8-Dimethoxy-10-methyl-5,10-dihydropyrrolo[1,2-*b*]isoquinolin-10-yl)acetonitrile (3a). According to General Procedure, *N*-(*o*-iodobenzyl)pyrrole **1a** (115 mg, 0.30 mmol) was treated with $Pd(OAc)_2$ (6.7 mg, 0.03 mmol), potassium hexacyanoferrate(II) trihydrate (27.9 mg, 0.07 mmol), sodium carbonate (41.3 mg, 0.39 mmol) and tetrabutylammonium chloride (83.4 mg, 0.30 mmol) in a 8/2 mixture of DMF/H_2O (1 mL) for 1 h. After workup, purification by column chromatography (silica gel, petroleum ether/EtOAc 8/2) afforded **3a** (54.9 mg, 65% yield) as a yellow solid: m. p. (petroleum ether/EtOAc): 132–134 °C. IR (ATR): 2935, 2245, 1515 cm^{-1}. ^1H NMR (300 MHz, $CDCl_3$): δ 7.05 (s, 1H), 6.75–6.74 (m, 2H), 6.26 (dd, J = 3.6, 2.7 Hz, 1H), 6.20 (dd, J = 3.6, 1.7 Hz, 1H), 5.18 (d, J = 15.9 Hz, 1H), 5.07 (d, J = 15.9 Hz, 1H), 3.95 (s, 3H), 3.90 (s, 3H), 2.72 (s, 2H), 1.88 (s, 3H). $^{13}C\{^1H\}$ NMR (75.5 MHz, $CDCl_3$): δ 148.6, 148.4, 132.5, 129.8, 124.0, 119.3, 117.8, 109.2, 108.8, 108.4, 103.5, 56.2, 56.0, 47.1, 37.5, 34.2, 26.4. MS (ESI) *m/z* (rel intensity): 283 (MH^+, 100), 242 (46). HRMS (ESI-TOF): calcd for $C_{17}H_{19}N_2O_2$ [MH^+] 283.1447; found, 283.1450.

2-(10-Methyl-5,10-dihydropyrrolo[1,2-*b*]isoquinolin-10-yl) acetonitrile (3b). According to General Procedure, *N*-(*o*-iodobenzyl)pyrrole **1b** (101 mg, 0.30 mmol) was treated with $Pd(OAc)_2$ (6.7 mg, 0.03 mmol), potassium hexacyanoferrate(II) trihydrate (27.9 mg, 0.07 mmol), sodium carbonate (41.3 mg, 0.39 mmol) and tetrabutylammonium chloride (83.4 mg, 0.30 mmol) in an 8/2 mixture of DMF/H_2O (1 mL) for 4 h. After workup, purification by column chromatography (silica gel, petroleum ether/EtOAc 95/5) afforded **3b** (17.4 mg, 23% yield) as a colorless oil: IR (ATR): 2925, 2250, 1515 cm^{-1}. ^1H NMR (300 MHz, $CDCl_3$): δ 7.59–7.56 (m, 1H), 7.40–7.28 (m, 3H), 6.76 (dd, J = 2.7, 1.7 Hz, 1H), 6.26 (dd, J = 3.6, 2.7 Hz, 1H), 6.21 (dd, J = 3.6, 1.7 Hz, 1H), 5.24 (d, J = 16.1 Hz, 1H), 5.14 (d, J = 16.1 Hz, 1H), 2.74 (s, 2H), 1.89 (s, 3H). $^{13}C\{^1H\}$ NMR (75.5 MHz, $CDCl_3$): δ 137.9, 132.4, 131.8, 128.1, 127.5, 126.6, 125.2, 119.4, 117.5, 108.8, 103.7, 47.5, 37.8, 33.8, 26.0. MS (ESI) *m/z* (rel intensity): 223 (MH^+, 65), 182 (100). HRMS (ESI-TOF): calcd for $C_{15}H_{15}N_2$ [MH^+] 223.1235; found, 223.1237.

2-(10-Methyl-5,10-dihydro-[1,3]dioxolo[4,5-*g*]pyrrolo[1,2-*b*] isoquinolin-10-yl)acetonitrile (3c). According to General Procedure, *N*-(*o*-iodobenzyl)pyrrole **1c** (110 mg, 0.30 mmol) was treated with $Pd(OAc)_2$ (6.7 mg, 0.03 mmol), potassium hexacyanoferrate(II) trihydrate (27.9 mg, 0.07 mmol), sodium carbonate (41.3 mg, 0.39 mmol) and tetrabutylammonium chloride (83.4 mg, 0.30 mmol) in a 8/2 mixture of DMF/H_2O (1 mL) for 1 h. After workup, purification by column chromatography (silica gel, petroleum ether/EtOAc 8/2) afforded **3c** (29.5 mg, 37% yield) as a yellow oil: IR (ATR): 2915, 2250, 1485 cm^{-1}. ^1H NMR (300 MHz, $CDCl_3$): δ 7.01 (s, 1H), 6.74–6.70 (m, 2H), 6.26–6.25 (m, 1H), 6.18 (dd, J = 3.7, 1.7 Hz, 1H), 6.00 (s, 2H), 5.15 (d, J = 15.9 Hz, 1H), 5.03 (d, J = 15.9 Hz, 1H), 2.73 (d, J = 16.4 Hz, 1H), 2.66 (d, J = 16.4 Hz, 1H), 1.84 (s, 3H). $^{13}C\{^1H\}$ NMR (75.5 MHz, $CDCl_3$): δ 147.6, 147.0, 132.3, 131.3, 125.3, 119.2, 117.5, 108.8, 106.4, 105.4, 103.6, 101.5, 47.5, 37.8, 34.0, 26.3. MS (ESI) *m/z* (rel intensity): 267 (MH^+, 100), 226 (76). HRMS (ESI-TOF): calcd for $C_{16}H_{15}N_2O_2$ [MH^+] 267.1134; found, 267.1137.

2-(6,7-Dimethoxy-10-methyl-5,10-dihydropyrrolo[1,2-*b*]isoquinolin-10-yl)acetonitrile (3d). According to General Procedure, *N*-(*o*-iodobenzyl)pyrrole **1d** (113 mg, 0.30 mmol) was treated with $Pd(OAc)_2$ (6.7 mg, 0.03 mmol), potassium hexacyanoferrate(II) trihydrate (27.9 mg, 0.07 mmol), sodium carbonate (41.3 mg, 0.39 mmol) and tetrabutylammonium chloride (83.4 mg, 0.30 mmol) in a 8/2 mixture of DMF/H_2O (1 mL) for 2 h. After workup, purification by column chromatography (silica gel, petroleum ether/EtOAc 9/1) afforded **3d** (32.4 mg, 39% yield) as a brown oil: IR (ATR): 2935, 2250, 1495 cm^{-1}. ^1H NMR (300 MHz, $CDCl_3$): δ 7.26 (d, J = 8.7 Hz, 1H), 6.96 (d, J = 8.7 Hz, 1H), 6.79–6.78 (m, 1H), 6.26–6.24 (m, 1H), 6.17 (dd, J = 3.6, 1.7 Hz, 1H), 5.35 (d, J = 16.9 Hz, 1H), 5.05 (d, J = 16.9 Hz, 1H), 3.91 (s, 3H), 3.90 (s, 3H), 2.70 (s, 2H), 1.86 (s, 3H). $^{13}C\{^1H\}$ NMR (75.5 MHz, $CDCl_3$): δ 151.2, 144.8, 132.5, 130.8, 126.1, 120.6, 119.7, 117.6, 111.7, 108.7, 103.4, 60.5, 55.8, 42.7, 37.4, 34.2, 26.1. MS (ESI) *m/z* (rel intensity): 283 (MH^+, 100), 242 (30). HRMS (ESI-TOF): calcd for $C_{17}H_{19}N_2O_2$ [MH^+] 283.1447; found, 283.1453.

2-(7,9-Dimethoxy-10-methyl-5,10-dihydropyrrolo[1,2-*b*]isoquinolin-10-yl)acetonitrile (3e). According to General Procedure, *N*-(*o*-iodobenzyl)pyrrole **1e** (115 mg, 0.30 mmol) was treated with $Pd(OAc)_2$ (6.7 mg, 0.03 mmol), potassium hexacyanoferrate(II) trihydrate (27.9 mg, 0.07 mmol), sodium carbonate (41.3 mg, 0.39 mmol) and tetrabutylammonium chloride (83.4 mg, 0.30 mmol) in a 8/2 mixture of DMF/H_2O (1 mL) for 48 h. After workup, purification by column chromatography (silica gel, petroleum ether/EtOAc 8/2) afforded **3e** (18.1 mg, 21% yield) (63% conversion) as a yellow solid: m. p. (petroleum ether/EtOAc): 167–169 °C. IR (ATR): 2935, 2250, 1460 cm^{-1}. ^1H NMR (300 MHz, $CDCl_3$): δ 6.68 (dd, J = 2.7, 1.7 Hz, 1H), 6.47 (d, J = 2.5 Hz, 1H), 6.35 (d, J = 2.5 Hz, 1H), 6.33 (dd, J = 3.7, 2.7 Hz, 1H), 6.20 (dd, J = 3.7, 1.7 Hz, 1H), 5.25 (d, J = 16.3 Hz, 1H), 5.13 (d, J = 16.3 Hz, 1H), 3.90 (s, 3H), 3.83 (s, 3H), 3.54 (d, J = 16.3 Hz, 1H), 2.97 (d, J = 16.3 Hz, 1H), 1.80 (s, 3H). $^{13}C\{^1H\}$ NMR (75.5 MHz, $CDCl_3$): δ 159.7, 159.2, 134.6, 133.6, 118.8, 117.9, 117.2, 109.3, 103.2, 102.2, 98.8, 55.4, 55.3, 47.2, 37.8, 31.5, 28.9. MS (ESI) *m/z* (rel intensity): 283 (MH^+, 100), 242 (33). HRMS (ESI-TOF): calcd for $C_{17}H_{19}N_2O_2$ [MH^+] 283.1447; found, 283.1440.

2-(7-Fluoro-10-methyl-5,10-dihydropyrrolo[1,2-*b*]isoquinolin-10-yl)acetonitrile (3f). According to General Procedure, *N*-(*o*-iodobenzyl)pyrrole **1f** (102 mg, 0.30 mmol) was treated with $Pd(OAc)_2$ (6.7 mg, 0.03 mmol), potassium hexacyanoferrate(II) trihydrate (27.9 mg, 0.07 mmol), sodium carbonate (41.3 mg, 0.39 mmol) and tetrabutylammonium chloride (83.4 mg, 0.30 mmol) in a 8/2 mixture of DMF/H_2O (1 mL) for 48 h. After workup, purification by column chromatography (silica gel, petroleum ether/EtOAc 9/1) afforded **3f** (11.8 mg, 16% yield) as a yellow oil: IR (ATR): 2925, 2250, 1500 cm^{-1}. ^1H NMR (300 MHz, $CDCl_3$): δ 7.57 (dd, J = 8.8, 5.3 Hz, 1H), 7.11 (td, J = 8.8, 2.7 Hz, 1H), 7.01 (dd, J = 8.8, 2.7 Hz, 1H), 6.78–6.77 (m, 1H), 6.29–6.21 (m, 2H), 5.25 (d, J = 16.3 Hz, 1H), 5.14 (d, J = 16.3 Hz, 1H), 2.80–2.68 (m, 2H), 1.90 (s, 3H). $^{13}C\{^1H\}$ NMR (75.5 MHz, $CDCl_3$): δ 161.6 (d, J = 247.5 Hz), 134.1 (d, J = 7.7 Hz), 133.7 (d, J = 3.3 Hz), 132.2, 127.2 (d, J = 8.3 Hz), 119.4, 117.4, 115.1 (d, J = 21.4 Hz), 113.3 (d, J = 22.4 Hz), 109.1, 103.9, 47.4 (d, J = 2.2 Hz), 37.6, 34.0, 26.2. MS (ESI) *m/z* (rel intensity): 241 (MH^+, 59), 200 (100). HRMS (ESI-TOF): calcd for $C_{15}H_{14}FN_2$ [MH^+] 241.1141; found, 241.1145.

2-(7-Methoxy-10-methyl-5,10-dihydropyrrolo[1,2-*b*]isoquinolin-10-yl)acetonitrile (3g). According to General Procedure, *N*-(*o*-iodobenzyl)pyrrole **1g** (106 mg, 0.30 mmol) was treated with $Pd(OAc)_2$ (6.7 mg, 0.03 mmol), potassium hexacyanoferrate(II) trihydrate (27.9 mg, 0.07 mmol), sodium carbonate (41.3 mg, 0.39 mmol) and tetrabutylammonium chloride (83.4 mg,

0.30 mmol) in a 8/2 mixture of DMF/H_2O (1 mL) for 6 h. After workup, purification by column chromatography (silica gel, petroleum ether/EtOAc 9/1) afforded **3g** (17.4 mg, 23% yield) (94% conversion) as a colorless oil: IR (ATR): 2930, 2250, 1500 cm^{-1}. ^1H NMR (300 MHz, $CDCl_3$): δ 7.50 (d, $J = 8.7$ Hz, 1H), 6.94 (dd, $J = 8.7$, 2.7 Hz, 1H), 6.80 (d, $J = 2.7$ Hz, 1H), 6.76 (dd, $J = 2.7$, 1.7 Hz, 1H), 6.27 (dd, $J = 3.7$, 2.7 Hz, 1H), 6.21 (dd, $J = 3.7$, 1.7 Hz, 1H), 5.23 (d, $J = 16.1$ Hz, 1H), 5.12 (d, $J = 16.1$ Hz, 1H), 3.85 (s, 3H), 2.73 (s, 2H), 1.88 (s, 3H). $^{13}C\{^1H\}$ NMR (75.5 MHz, $CDCl_3$): δ 158.6, 133.2, 132.8, 130.0, 126.5, 119.3, 117.6, 113.6, 111.6, 108.8, 103.6, 55.4, 47.6, 37.3, 34.1, 26.2. MS (ESI) *m/z* (rel intensity): 253 (MH^+, 94), 212 (100). HRMS (ESI-TOF): calcd for $C_{16}H_{17}N_2O$ [MH^+] 253.1341; found, 253.1339.

2-[7-(Benzyloxy)-10-methyl-5,10-dihydropyrrolo[1,2-*b*]isoquinolin-10-yl]acetonitrile (3h). According to General Procedure, *N*-(*o*-iodobenzyl)pyrrole **1h** (128 mg, 0.30 mmol) was treated with $Pd(OAc)_2$ (6.7 mg, 0.03 mmol), potassium hexacyanoferrate(II) trihydrate (27.9 mg, 0.07 mmol), sodium carbonate (41.3 mg, 0.39 mmol) and tetrabutylammonium chloride (83.4 mg, 0.30 mmol) in a 8/2 mixture of DMF/H_2O (1 mL) for 1 h. After workup, purification by column chromatography (silica gel, petroleum ether/EtOAc 98/2) afforded **3h** (22.5 mg, 23% yield) as a yellow oil: IR (ATR): 2975, 2245, 1500 cm^{-1}. ^1H NMR (300 MHz, $CDCl_3$): δ 7.50–7.35 (m, 6H), 7.01 (dd, $J = 8.7$, 2.7 Hz, 1H), 6.88 (d, $J = 2.6$ Hz, 1H), 6.75 (dd, $J = 2.7$, 1.7 Hz, 1H), 6.27 (dd, $J = 3.6$, 2.7 Hz, 1H), 6.21 (dd, $J = 3.6$, 1.7 Hz, 1H), 5.21 (d, $J = 16.0$ Hz, 1H), 5.11 (s, 2H), 5.10 (d, $J = 16.0$ Hz, 1H), 2.74 (d, $J = 16.4$ Hz, 1H), 2.70 (d, $J = 16.4$ Hz, 1H), 1.88 (s, 3H). $^{13}C\{^1H\}$ NMR (75.5 MHz, $CDCl_3$): δ 157.8, 136.7, 133.2, 132.7, 130.3, 128.7, 128.2, 127.5, 126.5, 119.3, 117.6, 114.5, 112.6, 108.8, 103.6, 70.2, 47.6, 37.3, 34.1, 26.2. MS (ESI) *m/z* (rel intensity): 329 (MH^+, 100), 288 (18). HRMS (ESI-TOF): calcd for $C_{22}H_{21}N_2O$ [MH^+] 329.1654; found, 329.1648.

2-[7-(Benzyloxy)-8-methoxy-10-methyl-5,10-dihydropyrrolo[1,2-*b*]isoquinolin-10-yl]acetonitrile (3i). According to General Procedure, *N*-(*o*-iodobenzyl)pyrrole **1i** (138 mg, 0.30 mmol) was treated with $Pd(OAc)_2$ (6.7 mg, 0.03 mmol), potassium hexacyanoferrate(II) trihydrate (27.9 mg, 0.07 mmol), sodium carbonate (41.3 mg, 0.39 mmol) and tetrabutylammonium chloride (83.4 mg, 0.30 mmol) in a 8/2 mixture of DMF/H_2O (1 mL) for 24 h. After workup, purification by column chromatography (silica gel, petroleum ether/EtOAc 98/2) afforded **3i** (16.7 mg, 16% yield) as a yellow oil: IR (ATR): 2930, 2250, 1510 cm^{-1}. ^1H NMR (300 MHz, $CDCl_3$): δ 7.48–7.32 (m, 5H), 7.09 (s, 1H), 6.76 (s, 1H), 6.73 (dd, $J = 2.7$, 1.7 Hz, 1H), 6.26 (dd, $J = 3.6$, 2.7 Hz, 1H), 6.19 (dd, $J = 3.7$, 1.7 Hz, 1H), 5.23 (s, 2H), 5.12 (d, $J = 15.8$ Hz, 1H), 5.00 (d, $J = 15.8$ Hz, 1H), 3.97 (s, 3H), 2.72 (s, 2H), 1.90 (s, 3H). $^{13}C\{^1H\}$ NMR (75.5 MHz, $CDCl_3$): δ 149.3, 147.6, 136.8, 132.4, 130.4, 128.7, 128.0, 127.2, 123.9, 119.3, 117.6, 111.9, 109.1, 108.7, 103.5, 71.2, 56.4, 47.1, 37.5, 34.2, 26.1. MS (ESI) *m/z* (rel intensity): 359 (MH^+, 100), 318 (6). HRMS (ESI-TOF): calcd for $C_{23}H_{23}N_2O_2$ [MH^+] 359.1760; found, 359.1760.

7.2. Biological assay details for the IC_{50} and CC_{50} determinations against the L. donovani and L. amazonensis

Parasites and culture procedure. The following species of *Leishmania* were used: *L. donovani* (MHOM/IN/80/DD8) was purchased (ATCC, USA) and *L. amazonensis* (MHOM/Br/79/Maria) were kindly provided by Prof. Alfredo Toraño (Instituto de Salud Carlos III, Madrid). Promastigotes were cultured in Schneider's Insect Medium supplemented with 10% heat-inactivated Foetal Bovine Serum (FBS) and 1000 U/L of penicillin plus 100 mg/L of streptomycin in 25 mL culture flasks at 26 °C.

***In vitro* promastigote susceptibility assay**. The assay was performed as previously described [35]. Briefly, log-phase promastigotes (2.5×10^5 parasites/well) were cultured in 96-well plastic plates. Stock solutions of the tested compounds were solubilized at 50 mg/mL in DMSO. Serial dilutions 1:2 of test compounds in fresh culture medium (100, 50, 25, 12.5, 6.25, 3.12, 1.56 and 0.78 μg/mL) were carried out up to 200 μL final volume. Growth control and signal-to-noise were also included. The final solvent (DMSO) concentrations never exceeded 0.5% (v/v) warranting no effect on parasites proliferation or morphology. After 48 h at 26 °C, 20 μL of a 2.5 mM resazurin solution was added to each well and the plates were returned to the incubator for another 3 h. The Relative Fluorescence Units (RFU) (535 nm–590 nm excitation-emission wavelength) was determined in a fluorometer (Infinite 200Tecan i-Control). Growth inhibition (%) was calculated by 100 - [(RFU treated wells − RFU signal-to-noise)/(RFU untreated − RFU signal-to-noise) x 100]. All tests were carried out in triplicate. Miltefosine (Sigma-Merck, Madrid, Spain) was used as reference drug and was evaluated under the same conditions. The efficacy of each compound was estimated by calculating the IC_{50} (concentration of the compound that produced a 50% reduction in parasites) using a multinomial probit analysis incorporated in SPSS software v21.0. The selectivity index (SI) was calculated as the ratio between cytotoxicity (CC_{50}) and activity against parasites (IC_{50}).

***In vitro* intracellular amastigote susceptibility assay**. The assay was carried out as previously described [36]. Briefly, 5×10^4 J774 macrophages and stationary promastigotes in a 1:5 ratio was seeded in each well of a microtiter plate, suspended in 200 μL of culture medium and incubated for 24 h at 33 °C in 5% CO_2 chamber. After this first incubation, the temperature was increased up to 37 °C for another 24h. Thereafter, cells were washed several times in culture medium by centrifugation at 1.500*g* for 5 min in order to remove free non-internalized promastigotes. Finally, the supernatant was replaced by 200 μL/well of culture medium containing 2-fold serial dilutions of the test compounds as in promastigotes assay. Growth control and signal-to-noise were also included. Following incubation for 48 h at 37 °C, 5% CO_2, the culture medium was replaced by 200 μL/well of the lysis solution (RPMI-1640 with 0.048% HEPES and 0.01% SDS) and incubated at room temperature for 20 min. Thereafter, the plates were centrifuged at 3.500*g* for 5 min and the lysis solution was replaced by 200 μL/well of Schneider's insect medium. The culture plates were then incubated at 26 °C for other 4 days to allow transformation of viable amastigotes into promastigotes and proliferation. Afterwards, 20 μL/well of 2.5 mM resazurin was added and incubated for another 3 h. Finally, fluorescence emission was measured and IC_{50} was estimated as described above. All tests were carried out in triplicate. Miltefosine (Sigma-Merck, Madrid, Spain) was used as reference drug and was evaluated at the same conditions. The IC_{50} and SI were calculated as in previous section.

Cytotoxicity assay on macrophages. The assay was carried out as previously described [37]. J774 macrophages cell lines were seeded (5×10^4 cells/well) in 96-well flat-bottom microplates with 100 μL of RPMI 1640 medium. The cells were allowed to attach for 24 h at 37 °C, 5% CO_2, and the medium was replaced by different concentrations of the compounds in 200 μL of medium and exposed for another 24 h. Growth controls and signal-to-noise were also included. Afterwards, a volume of 20 μL of the 2.5 mM resazurin solution was added, and plates were returned to the incubator for another 3 h to evaluate cell viability. The reduction of resazurin was determined by fluorometry as in the promastigote assay. Each concentration was assayed three times. Cytotoxicity effect of compounds was defined as the 50% reduction of cell viability of treated culture cells with respect to untreated culture (CC_{50}) and was calculated using a multinomial probit analysis incorporated in SPSS software v21.0.

7.3. Computational methods

A PTML model has been developed for prediction of the probability $p(f(v_{ij})_{obs} = 1)$ with which the experimental values v_{ij} of biological activity the drug tested under the assay conditions reach a desired level $f(v_{ij})_{obs} = 1$ or not $f(v_{ij})_{obs} = 0$. The general workflow for the PTML involves the following general steps: (1) data download, (2) data pre-processing, (3) training and validation of the model, and (4) application of the model for predictive study. The step (2) includes the following operations: (2a) calculation of objective function, (2b) calculation of function of reference, and (2c) calculation of Perturbation-Theory Operators (PTOs). The different steps are explained in the SI section.

PTML model data download and pre-processing. First, a dataset of 145,851 preclinical assays of putative antileishmanial compounds were downloaded from ChEMBL. All experimental values of biological properties v_{ij} were transformed into a categorical objective function $f(v_{ij})_{obs}$, in order to minimize accuracy problems. The structure of the drugs was codified using a vector of molecular descriptors D_{ki} for each drug. The elements of this vector are the numeric values of the different the molecular descriptors D_{ki} of each drug. As stated in the Result section, the descriptors $D_1 = ALOGP$, $D_2 = PSA$, and $D_3 = NRV$ were used used to identify the compound in the equation. The values of D_k were extracted from ChEMBL dataset and/or calculated with the software DRAGON in the case of new compounds. Next, the assay conditions were codified using a vector of conditions c_j (see details in next section). Due to the high number of different biological parameters with different scales and levels of errors, they were discretized by the Boolean function $f(v_{ij})_{obs}$ obtained to develop a classification model. Next, PT Operators (PTOs) were calculated in order to zip into a single variable information about both the structure of the drug (D_k vectors) and the biological assay carried out (c_j vectors). Then, PTOs were defined by 10 different boundary conditions, labels, or discrete variables of each assay c_1, c_2, c_3, …, c_{10}. The PTOs have the following form: $\Delta D_k(c_j) = D_k - \langle D_k(c_j)\rangle$. These operators quantify the deviation (Δ) of the molecular descriptors of a given compound D_k (structure) with respect to the expected values $\langle D_k(c_j)\rangle$ of these descriptors for all the compounds previously assayed under the same conditions c_j.

PTML linear model. PTML modeling technique is useful to seek predictive models for complex datasets with multiple Big Data features [38,19a]. We can predict the posterior probability $p(f(v_{ij}) = 1)$ with which the the query compound reach the desired level of activity $f(v_{ij})_{obs} = 1$ in the the preclinical assay with an specific sub-set of conditions of assay selected out of multiple conditions of assay $c_j = (c_0, c_1, c_2, \ldots c_{jmax})$. PTOs similar to Box-Jenkins MA operators, are used as input [39,19a]. PTML linear models have the following form:

$$f(v_{ij})_{calc} = a_0 + a_1 \cdot f(v_{ij})_{ref} + \sum_{k=1}^{k_{max}} \sum_{j=0}^{j_{max}} a_{kj} \cdot \Delta D_k(c_j)$$

The output of the model is a dimensionless parameter $f(v_{ij})_{calc}$, which can be easily transformed into the wanted probabilities $p(f(v_{ij}) = 1)$ using a sigmoid function. The first input variable is the function of reference $f(v_{ij})_{ref}$. It is the prior expected probability with which a random reference compound may have the desired level of activity for the biological parameter c_0. PTOs have been calculated for all descriptors D_k with respect two types of experimental conditions c_I and c_{II} (subsets) of categorical variables. They have been created to encode separately information about experimental conditions of preclinical assays (c_I) or about the nature and quality of data (c_{II}). The first partition c_I, or sub-set of conditions, includes conditions related to the system of assay *per se*, target protein, cell line, organism, *etc*., while the conditions/labels of assay collected in the second partition c_{II} are related to the nature and quality of data. Numerous examples of numerical values of c_0, $f(v_{ij})_{ref}$, and $\langle D_k(c_I)\rangle$ and $\langle D_k(c_J)\rangle$ for many assay conditions have been included in Tables S6, S7 and S8 of the Supplementary Material.

PTML model prediction of new results. Computational prediction of the outcomes of 19 compounds of our series *vs*. >20 *Leishmania* species in more than 70 different preclinical assays were carried out using the new PTML model. The values of the $f(v_{ij})_{ref}$ and the PTOs ($\Delta D_k(c_j) = D_k - \langle D_k(c_j)\rangle$) for each compound in different assays were substituted into the equation. The values $\langle D_k(c_j)\rangle$ are the average values of the descriptors D_k for all the compounds previously assayed under the same conditions c_j. Consequently, they can be used indirectly to define the specific conditions of assay we want to predict [17]. After substituting the values D_k for each compound and the values of $f(v_{ij})_{ref}$ and $\langle D_k(c_j)\rangle$ for each assay, the values of the output function $f(v_{ij})_{calc}$ were obtained. Next, these values were transformed into probabilities using a sigmoid function, see details in SI. Thus, once the posterior values of probabilities have been calculated, the compounds can be classified. Those compounds in the range of probability $p(f(v_{ij})_{pred} = 1) > 0.5$ are considered interesting for assay $f(v_{ij})_{pred} = 1$.

Declaration of competing interest

The authors declare that they have no known competing financial interests or personal relationships that could have appeared to influence the work reported in this paper.

Acknowledgment

Ministerio de Economía y Competitividad (CTQ2016-74881-P), Ministerio de Ciencia e Innovación (PID2019-104148 GB-I00) and Gobierno Vasco (IT1045-16) are gratefully acknowledged for their financial support. I. B. wishes to thank Fundación Biofísica Bizkaia/Biofisika Bizkaia Fundazioa (FBB) for a postdoctoral grant. Technical and human support provided by Servicios Generales de Investigación SGIker (UPV/EHU, MINECO, GV/EJ, ERDF and ESF) is also acknowledged.

Appendix A. Supplementary data

Supplementary data to this article can be found online at https://doi.org/10.1016/j.ejmech.2021.113458.

References

[1] World Health Organization (WHO)/Department of Control of Neglected Tropical Diseases, Leishmaniasis in high-burden countries: an epidemiological update based on data reported in. https://www.who.int/leishmaniasis/resources/who_wer9122/en/, 2014. (Accessed 10 February 2021).

[2] [a] A. Schwing, C. Pomares, A. Majoor, L. Boyer, P. Marty, G. Michel, Leishmania infection: misdiagnosis as cancer and tumor-promoting potential, Acta Trop. 197 (2019) 104855, https://doi.org/10.1016/j.actatropica.2018.12.010;
[b] H. Akuffo, C. Costa, J. van Griensven, S. Burza, J. Moreno, M. Herrero, New insights into leishmaniasis in the immunosuppressed, PLoSNegl Trop Dis 12 (2018), e0006375, https://doi.org/10.1371/journal.pntd.0006375.

[3] [a] S. Sundar, J. Chakravarty, Leishmaniasis: an update of current pharmacotherapy, Expet Opin. Pharmacother. 14 (2013) 53–63, https://doi.org/10.1517/14656566.2013.755515. See also;
[b] N.G. Jones, C.M.C. Catta-Preta, A.P.C.A. Lima, J.C. Mottram, Genetically validated drug targets in Leishmania: current knowledge and future prospects, ACS Infect. Dis. 4 (2018) 467–477, https://doi.org/10.1021/acsinfecdis.7b00244.

[4] S. Sundar, A. Singh, Chemotherapeutics of visceral leishmaniasis: present and future developments, Parasitology 145 (2018) 481–489, https://doi.org/

10.1017/S0031182017002116.
[5] T.P. Dorlo, M. Balasegaram, J.H. Beijnen, P.J. de Vries, Miltefosine: a review of its pharmacology and therapeutic efficacy in the treatment of leishmaniasis, J. Antimicrob. Chemother. 67 (2012) 2576–2597, https://doi.org/10.1093/jac/dks275.
[6] [a] S. Sundar, J. Chakravarty, Leishmaniasis: an update of current pharmacotherapy, Expet Opin. Pharmacother. 14 (2013) 53–63, https://doi.org/10.1517/14656566.2013.755515;
[b] P. Bilbao-Ramos, M.A. Dea-Ayuela, O. Cardenas-Alegría, E. Salamanca, J.A. Santalla-Vargas, C. Benito, N. Flores, F. Bolás-Fernández, Leishmaniasis in the major endemic region of Plurinational State of Bolivia: species identification, phylogeography and drug susceptibility implications, Acta Trop. 176 (2017) 150–161, https://doi.org/10.1016/j.actatropica.2017.07.026.
[7] P. Minodier, P. Parola, Cutaneous leishmaniasis treatment, Trav. Med. Infect. Dis. 5 (2007) 150–158, https://doi.org/10.1016/j.tmaid.2006.09.004.
[8] [a] S. Wyllie, M. Thomas, S. Patterson, et al., Nature 560 (2018) 192–197, https://doi.org/10.1038/s41586-018-0356-z;
[b] M.G. Thomas, M. De Rycker, M. Ajakane, S. Albrecht, et al., Identification of GSK3186899/DDD853651 as a preclinical development candidate for the treatment of visceral leishmaniasis, J. Med. Chem. 62 (2019) 1180–1202, https://doi.org/10.1021/acs.jmedchem.8b01218.
[9] [a] S. Khare, A.S. Nagle, A. Biggart, et al., Proteasome inhibition for treatment of leishmaniasis, Chagas disease and sleeping sickness, Nature 537 (2016) 229–233, https://doi.org/10.1038/nature19339;
[b] A. Nagle, A. Biggart, C. Be, H. Srinivas, H, et al., Discovery and characterization of clinical candidate LXE408 as a Kinetoplastid-selective proteasome inhibitor for the treatment of leishmaniases, J. Med. Chem. 63 (2020) 10773–10781, https://doi.org/10.1021/acs.jmedchem.0c00499.
[10] P.M. Loiseau, S. Cojean, J. Schrével, Sitamaquine as a putative antileishmanial drug candidate: from the mechanism of action to the risk of drug resistance, Parasite 18 (2011) 115–119, https://doi.org/10.1051/parasite/2011182115.
[11] [a] M. Staderini, M. Piquero, M.A. Abnegózar, M. Nachér-Vázquez, G. Romanelli, P. López-Alvarado, L. Rivas, M.L. Bolognesi, J.C. Menéndez, Structure-activity relationships and mechanistic studies of novel mitochondria-targeted, leishmanicidal derivatives of the 4-aminostyrylquinoline scaffold, Eur. J. Med. Chem. 171 (2019) 38–53, https://doi.org/10.1016/j.ejmech.2019.03.007;
[b] A. Upadhyay, P. Chandrakar, S. Gupta, N. Parmar, S.K. Singh, M. Rashid, P. Kushwaha, M. Wahajuddin, K.V. Sashidhara, S. Kar, Synthesis, biological evaluation, structure-activity relationship, and mechanism of action studies of quinoline-metronidazole derivatives against experimental visceral leishmaniasis, J. Med. Chem. 62 (2019) 5655–5671, https://doi.org/10.1021/acs.jmedchem.9b00628;
[c] S.Y. Bhat, P. Jagruthi, A. Srinivas, M. Arifuddin, I.A. Qureshi, Synthesis and characterization of quinoline-carbaldehyde derivatives as novel inhibitors for leishmanial methionine aminopeptidase, Eur. J. Med. Chem. 186 (2020) 111860, https://doi.org/10.1016/j.ejmech.2019.111860;
[d] D. Mukherjee, Md Yousuf, S. Dey, S. Chakraborty, A. Chaudhuri, V. Kumar, B. Sarkar, S. Nath, A. Hussain, A. Dutta, T. Mishra, B.G. Roy, S. Singh, S. Chakraborty, S. Adhikari, C. Pal, Targeting the Trypanothione reductase of tissue-residing Leishmania in hosts' reticuloendothelial system: a flexible water soluble ferrocenylquinoline-based preclinical drug candidate, J. Med. Chem. 63 (2020) 15621–15638, https://doi.org/10.1021/acs.jmedchem.0c00690.
[12] S. Hendrickx, G. Caljon, L. Maes, Need for sustainable approaches in anti-leishmanial drug discovery, Parasitol. Res. 118 (2019) 2743–2752, https://doi.org/10.1007/s00436-019-06443-2.
[13] (For some representative examples, see:). [a] U. Martínez Estíbalez, N. Sotomayor, E. Lete, Intramolecular carbolithiation reactions for the synthesis of 2,4-disubstituted tetrahydroquinolines. Evaluation of TMEDA and (-)-sparteine as ligands in the stereoselectivity, Org. Lett. 11 (2009) 1237–1240, https://doi.org/10.1021/ol900066c;
[b] S. Lage, U. Martínez Estíbalez, N. Sotomayor, E. Lete, Intramolecular palladium-catalyzed direct arylation vs. Heck reactions: synthesis of pyrroloisoquinolines and isoindoles, Adv. Synth. Catal. 351 (2009) 2460–2468, https://doi.org/10.1002/adsc.200900368;
[c] E. Coya, N. Sotomayor, E. Lete, Intramolecular direct arylation and Heck reactions in the formation of medium sized rings. Selective synthesis of fused indolizine, pyrroloazepine and pyrroloazocine systems, Adv. Synth. Catal. 356 (2014) 1853–1865, https://doi.org/10.1002/adsc.201400075;
[d] V. Ortiz de Elguea, N. Sotomayor, E. Lete, Two consecutive Pd(II)-promoted C-H alkenylation reactions for the synthesis of substituted 3-alkenylquinolones, Adv. Synth. Catal. 357 (2015) 463–473, https://doi.org/10.1002/adsc.201400931;
[e] A. Carral-Menoyo, L. Sotorrios, V. Ortiz-de-Elguea, A. Díaz-Andrés, N. Sotomayor, E. Gómez-Bengoa, E. Lete, Intramolecular Palladium(II)-catalyzed 6-endo C-H Alkenylation directed by the remote N-protecting Group. Mechanistic insight and application to the synthesis of dihydroquinolines, J. Org. Chem. 85 (2020) 2486–2503, https://doi.org/10.1021/acs.joc.9b03174.
[14] (For selected reviews, see:). [a] A. Evidente, A. Kornienko, Anticancer evaluation of structurally diverse Amaryllidaceae alkaloids and their synthetic derivatives, Phytochemistry Rev. 8 (2009) 449–459, https://doi.org/10.1007/s11101-008-9119-z;
[b] M.F. Pereira, C. Rochais, P. Dallemagne, Recent advances in phenanthroindolizidine and phenanthroquinolizidine derivatives with anticancer activities, Anti Canc. Agents Med. Chem. 15 (2015) 1080–1091, https://doi.org/10.2174/1871520615666150520143600;
[c] N. Cortés, R.A. Posada-Duque, R. Álvarez, F. Alzate, S. Berkov, G.P. Cardona-Gómez, E. Osorio, Neuroprotective activity and acetylcholinesterase inhibition of five Amaryllidaceae species: a comparative study, Life Sci. 122 (2015) 42–50, https://doi.org/10.1016/j.lfs.2014.12.011;
[d] M. He, C. Qu, O. Gao, X. Hu, X. Hong, Biological and pharmacological activities of Amaryllidaceae alkaloids, RSC Adv. 5 (2015) 16562–16574, https://doi.org/10.1039/C4RA14666B;
[e] J.J. Nair, J. van Staden, J. Bastida, Apoptosis-inducing effects of Amaryllidaceae alkaloids, Curr. Med. Chem. 23 (2016) 161–185;
[f] G. Zhan, J. Zhou, J. Liu, J. Huang, H. Zhang, R. Liu, G. Yao, Acetylcholinesterase inhibitory alkaloids from the whole plants of zephyranthescarinata, J. Nat. Prod. 80 (2017) 2462–2471, https://doi.org/10.1021/acs.jnatprod.7b00301.
[15] [a] E.J. Osorio, S.M. Robledo, J. Bastida, Alkaloids with antiprotozoal activity, in: G.A. Cordell (Ed.), The Alkaloids, vol. 66, Elsevier, San Diego, 2008, pp. 113–190, https://doi.org/10.1016/S1099-4831(08)00202-2 (Chapter 2);
[b] G. Prabhu, S. Agarwal, V. Sharma, S.M. Madurkar, P. Munshi, S. Singh, S. Sen, A natural product based DOS library of hybrid systems, Eur. J. Med. Chem. 95 (2015) 41–48, https://doi.org/10.1016/j.ejmech.2015.03.023;
[c] J.J. Nair, J. van Staden, Antiplasmodial lycorane alkaloid principles of the plant family Amaryllidaceae, Planta Med. 85 (2019) 637–647, https://doi.org/10.1055/a-0880-5414.
[16] [a] A. Ponte-Sucre, T. Gulder, A. Wegehaupt, C. Albert, C. Rikanović, L. Schaeflein, A. Frank, M. Schultheis, M. Unger, U. Holzgrabe, G. Bringmann, H. Moll, Structure-activity relationship and studies on the molecular mechanism of leishmanicidal N,C-coupled arylisoquinolinium salts, J. Med. Chem. 52 (2009) 626–636, https://doi.org/10.1021/jm801084u. See also;
[b] G. Bringmann, S.K. Bischof, S. Müller, T. Gulder, C. Winter, A. Stich, H. Moll, M. Kaiser, R. Brun, J. Dreher, K. Bauman, QSAR guided synthesis of simplified antiplasmodial analogs of naphthylisoquinoline alkaloids, Eur. J. Med. Chem. 45 (2010) 5370–5383, https://doi.org/10.1016/j.ejmech.2010.08.062.
[17] I. Barbolla, N. Sotomayor, E. Lete, Carbopalladation/suzuki coupling cascade for the generation of quaternary centers. Access to pyrrolo[1,2-*b*]isoquinolines, J. Org. Chem. 84 (2019) 10183–10196, https://doi.org/10.1021/acs.joc.9b01357.
[18] (For recent reviews, see:). [a] J. Biemolt, E. Ruijter, Advances in palladium-catalyzed cascade cyclizations, Adv. Synth. Catal. 360 (2018) 3821–3871, https://doi.org/10.1002/adsc.201800526;
[b] Y. Ping, Y. Li, J. Zhu, W. Kong, Construction of quaternary stereocenters by palladium-catalyzed carbopalladation-initiated cascade reactions, Angew. Chem. Int. Ed. 58 (2019) 1562–1573, https://doi.org/10.1002/anie.201806088;
[c] I. Barbolla, E. Lete, N. Sotomayor, Intramolecular mizoroki-heck reaction in the synthesis of heterocycles: strategies for the generation of tertiary and quaternary stereocenters, For examples of our work in the area; see, in: O. Attanasi, P. Merino, D. Spinelli (Eds.), Targets in Heterocyclic Systems, vol. 23Società Chimica Italiana, Roma, 2019, pp. 340–362 (Chapter 17), https://www.soc.chim.it/it/libri_collane/ths/vol_23_2019;
[d] E. Coya, N. Sotomayor, E. Lete, Enantioselective palladium catalyzed Heck-Heck cascade reactions. Ready access to the tretracyclic core of lycorane alkaloids, Adv. Synth. Catal. 357 (2015) 3206–3214, https://doi.org/10.1002/adsc.201500431;
[e] C. Blázquez-Barbadillo, E. Aranzamendi, E. Coya, E. Lete, N. Sotomayor, H. González-Díaz, Perturbation theory model of reactivity and enantioselectivity of palladium-catalyzed Heck-Heck cascade reactions, RSC Adv. 6 (2016) 38602–38610, https://doi.org/10.1039/C6RA08751E.
[19] (For selected reviews, see:). [a] H. González-Díaz, S. Arrasate, A. Gómez-San-Juan, S. Sotomayor, E. Lete, L. Besada-Porto, J.M. Ruso, General theory for multiple input-output perturbations in complex molecular systems. 1. Linear QSPR electronegativity models in physical, organic, and medicinal chemistry, Curr. Top. Med. Chem. 13 (2013) 1713–1741, https://doi.org/10.2174/15680266113134140011;
[b] H. González-Díaz, S. Arrasate, N. Sotomayor, E. Lete, C.R. Munteanu, A. Pazos, L. Besada-Porto, J.M. Ruso, MIANN models in medicinal, physical and organic chemistry, Curr. Top. Med. Chem. 13 (2013) 619–641, https://doi.org/10.2174/15680266113134050006;
[c] B. Ortega-Tenezaca, V. Quevedo-Tumailli, H. Bediaga, J. Collados, S. Arrasate, G. Madariaga, C.R. Munteanu, M.N.D.S. Cordeiro, H. González-Díaz, PTML multi-label algorithms: models, software, and applications, Curr. Top. Med. Chem. 20 (2020) 2326–2337, https://doi.org/10.2174/1568026620666200916122616.
[20] (For recent representative examples of our work in this area, see:). [a] J. Ferreira da Costa, D. Silva, O. Caamano, J.M. Brea, M.I. Loza, C.R. Munteanu, A. Pazos, X. García-Mera, H. González-Díaz, H. Perturbation theory/machine learning model of ChEMBL data for dopamine targets: docking, synthesis, and assay of new l-Prolyl-l-leucyl-glycinamide peptidomimetics, ACS Chem. Neurosci. 9 (2018) 2572–2587, https://doi.org/10.1021/acschemneuro.8b00083;
[b] R. Díez-Alarcia, V. Yañez-Pérez, I. Muneta Arrate, S. Arrasate, E. Lete, J.J. Meana, H. González-Díaz, Big data challenges targeting proteins in GPCR signaling pathways; combining PTML-ChEMBL models and [35S]GTPgammaS binding assays, ACS Chem. Neurosci. 10 (2019) 4476–4491, https://doi.org/

10.1021/acschemneuro.9b00302;
[c] D. Nocedo-Mena, C. Cornelio, M.R. Camacho-Corona, E. Garza-González, N.H. Waksman, S. Arrasate, N. Sotomayor, E. Lete, H. González-Díaz, Modeling antibacterial activity with machine learning and fusion of chemical structure information with microorganism metabolic networks, J. Chem. Inf. Model. 59 (2019) 1109–1120, https://doi.org/10.1021/acs.jcim.9b00034;
[d] R. Santana, R. Zuluaga, P. Gañán, S. Arrasate, E. Onieva, H. González-Díaz, PTML model of ChEMBL compounds assays for vitamin derivatives, ACS Comb. Sci. 22 (2020) 129–141, https://doi.org/10.1021/acscombsci.9b00166;
[e] R. Santana, R. Zuluaga, P. Gañán, S. Arrasate, E. Onieva, H. González-Díaz, Predicting coated-nanoparticle drug release systems with perturbation-theory machine learning (PTML) models, Nanoscale 12 (2020) 13471–13483, https://doi.org/10.1039/d0nr01849j.

[21] [a] R. Grigg, V. Santhakumar, V. Sridharan, Palladium catalysed cascade cyclisation - cyanide ion capture, Tetrahedron Lett. 34 (1993) 3163–3164, https://doi.org/10.1016/S0040-4039(00)60156-9. For a review, see;
[b] R. Grigg, V. Sridharan, Palladium catalyzed cascade cyclization-anion capture, relay switches and molecular queues, J. Organomet. Chem. 576 (1999) 65–87, https://doi.org/10.1016/S0022-328X(98)01052-3.

[22] [a] S. Jaegli, J.P. Vors, L. Neuville, J. Zhu, Total synthesis of horsfiline: a palladium-catalyzed domino heck-cyanation strategy, Synlett (2009) 2997–2999, https://doi.org/10.1055/s-0029-1218004;
[b] S. Jaegli, J.P. Vors, L. Neuville, J. Zhu, Palladium-catalyzed domino Heck/cyanation: synthesis of 3-cyanomethyloxindoles and their conversion to spirooxoindoles, Tetrahedron 66 (2010) 8911–8921, https://doi.org/10.1016/j.tet.2010.09.056.

[23] H. Yoon, D.A. Petrone, M. Lautens, Diastereoselective palladium-catalyzed arylcyanation/heteroarylcyanation of enantioenriched *N*-allylcarboxamides, Org. Lett. 16 (2014) 6420–6423, https://doi.org/10.1021/ol503243a.

[24] D.A. Petrone, A. Yen, N. Zeidan, M. Lautens, Dearomative indole bisfunctionalization via a diastereoselective palladium-catalyzed arylcyanation, Org. Lett. 17 (2015) 4838–4841, https://doi.org/10.1021/acs.orglett.5b02403.

[25] T. Schareina, A. Zapf, M. Beller, Potassium hexacyanoferrate(II)-A new cyanating agent for the palladium-catalyzed cyanation of aryl halides, Chem. Commun. (2004) 1388–1389, https://doi.org/10.1039/B400562G.

[26] [a] M. Sundermeier, A. Zapf, S. Mutyala, W. Baumann, J. Sans, S. Weiss, M. Beller, Progress in the palladium-catalyzed cyanation of aryl chlorides, Chem. Eur J. 9 (2003) 1828–1836, https://doi.org/10.1002/chem.200390210;
[b] R. Gerber, M. Oberholzer, C.M. Frech, Cyanation of aryl bromides with K4 [Fe(CN)6] catalyzed by dichloro[bis{1-(dicyclohexylphosphanyl)piperidine}] palladium, a molecular source of nanoparticles, and the reactions involved in the catalyst-deactivation processes, Chem. Eur J. 18 (2012) 2978–2986, https://doi.org/10.1002/chem.201102936.

[27] I.P. Beletskaya, A.V. Cheprakov, The Heck reaction as a sharpening stone of palladium catalysis, Chem. Rev. 100 (2000) 3009–3066, https://doi.org/10.1021/cr9903048.

[28] See, for example: C. Amatore, A. Jutand, Anionic Pd(0) and Pd(II) intermediates in palladium-catalyzed Heck and cross-coupling reactions Acc. Chem. Res. 33 (2000) 314–321, https://doi.org/10.1021/ar980063a.

[29] (See for example:). [a] M. Ortalli, S. Varani, G. Cimato, R. Veronesi, A. Quintavalla, M. Lombardo, M. Monari, C. Trombini, Evaluation of the pharmacophoric role of the O–O bond in synthetic antileishmanial compounds: comparison between 1,2- dioxanes and tetrahydropyrans, J. Med. Chem. 63 (2020) 13140–13158, https://doi.org/10.1021/acs.jmedchem.0c01589;
[b] M.G. Thomas, M. De Rycker, R.J. Wall, D. Spinks, O. Epemolu, S. Manthri, S. Norval, M. Osuna-Cabello, S. Patterson, J. Riley, F.R.C. Simeons, L. Stojanovski, J. Thomas, S. Thompson, C. Naylor, J.M. Fiandor, P.G. Wyatt, M. Marco, S. Wyllie, K.D. Read, T.J. Miles, I.H. Gilbert, Identification and optimization of a series of 8-hydroxy naphthyridines with potent in vitro antileishmanial activity: initial SAR and assessment of in vivo activity, J. Med. Chem. 63 (2020) 9523–9539, https://doi.org/10.1021/acs.jmedchem.0c00705.

[30] L.E. Kemp, M. Yamamoto, D. Soldati-Favre, Subversion of host cellular functions by the apicomplexan parasites, FEMS Microbiol. Rev. 37 (2013) 607–631, https://doi.org/10.1111/1574-6976.12013.

[31] R. Todeschini, V. Consonni, Handbook of molecular descriptors, in: R. Mannhold, H. Kubinyi, H. Timmerman (Eds.), Series: Methods and Principles in Medicinal Chemistry, Wiley-VCH, Weinheim, 2000, https://doi.org/10.1002/9783527613106.

[32] [a] M.C. Taylor, J.M. Kelly, C.J. Chapman, A.H. Fairlamb, M.A. Miles, The structure, organization, and expression of the Leishmania donovani gene encoding Trypanothione reductase, Mol. Biochem. Parasitol. 64 (1994) 293–301, https://doi.org/10.1016/0166-6851(94)00034-4;
[b] C. Chan, H. Yin, J. Garforth, J.H. McKie, R. Jaouhari, P. Speers, K.T. Douglas, P.J. Rock, V. Yardley, S.L. Croft, A.H. Fairlamb, Phenothiazine inhibitors of Trypanothione reductase as potential antitrypanosomal and antileishmanial drugs, J. Med. Chem. 41 (1998) 148–156, https://doi.org/10.1021/jm960814j.

[33] D. Ingrosso, A.V. Fowler, J. Bleibaum, S. Clarke, Sequence of the D-aspartyl/L-isoaspartyl protein methyltransferase from human erythrocytes. Common sequence motifs for protein, DNA, RNA, and small molecule *S*-Adenosylmethionine-Dependent methyltransferases, J. Biol. Chem. 264 (1989) 20131–20139, https://doi.org/10.1016/S0021-9258(19)47228-1.

[34] S. Hanson, J. Adelman, B. Ullman, Amplification and molecular cloning of the ornithine decarboxylase gene of Leishmania donovani, J. Biol. Chem. 267 (1992) 2350–2359, https://doi.org/10.1016/S0021-9258(18)45885-1.

[35] [a] P. Bilbao-Ramos, C. Galiana-Roselló, M.A. Dea-Ayuela, M. González-Alvarez, C. Vega, M. Rolón, J. Pérez-Serrano, F. Bolás-Fernández, M.E. González-Rosende, Nuclease activity and ultrastructural effects of new sulfonamides with anti-leishmanial and trypanocidal activities, Parasitol. Int. 61 (2012) 604–613, https://doi.org/10.1016/j.parint.2012.05.015. See also;
[b] M.A. Dea-Ayuela, P. Bilbao-Ramos, F. Bolás-Fernández, M.A. González-Cardenete, Synthesis and antileishmanial activity of C7- and C12-functionalized dehydroabietylamine derivatives, Eur. J. Med. Chem. 121 (2016) 445–450.

[36] P. Bilbao-Ramos, S. Sifontes-Rodríguez, M.A. Dea-Ayuela, F. Bolás-Fernández, A. fluorometric method for evaluation of pharmacological activity against intracellular Leishmania amastigotes, J. Microbiol. Methods 89 (2012) 8–11, https://doi.org/10.1016/j.mimet.2012.01.013.

[37] C. Galiana-Roselló, P. Bilbao-Ramos, M.A. Dea-Ayuela, M. Rolón, C. Vega, F. Bolás-Fernández, E. García-España, J. Alfonso, C. Coronel, M.E. González-Rosende, In vitro and in vivo antileishmanial and trypanocidal studies of new *N*-benzene- and *N*-naphthalenesulfonamide derivatives, J. Med. Chem. 56 (2013) 8984–8998, https://doi.org/10.1021/jm4006127.

[38] H. González-Díaz, L.G. Pérez-Montoto, F.M. Ubeira, Model for vaccine design by prediction of B-epitopes of IEDB given perturbations in peptide sequence, in vivo process, experimental techniques, and source or host organisms, J. Immunol. Res. (2014) 768515, https://doi.org/10.1155/2014/768515, 2014.

[39] S.G. Martínez-Arzate, E. Tenorio-Borroto, A. Barbabosa Pliego, H.M. Díaz-Albiter, J.C. Vázquez-Chagoyán, H. González-Díaz, PTML model for proteome mining of B-cell epitopes and theoretical-experimental study of Bm86 protein sequences from colima, Mexico, J. Proteome Res. 16 (2017) 4093–4103, https://doi.org/10.1021/acs.jproteome.7b00477.